NATIONAL TECHNICAL UNIVERSITY OF ATHENS
SCHOOL OF CHEMICAL ENGINEERING
LABORATORY OF INORGANIC MATERIALS TECHNOLOGY

DIPLOMA THESIS

Title

BIO-DEGRADATION OF PLASTIC POLUTANTS ACTIVATED THROUGH SONOCHEMICAL, PHOTOCATALYTIC AND PLASMA TECHNIQUES

by

NIKOLAOS PAPADIMITRIOU

Registration Number: 05117102

Supervisor: Prof. Dr.-Ing. Christos Argirusis

ATHENS, September 2022

ACKNOWLEDGMENTS

The present thesis was conducted in collaboration between the School of Chemical Engineering of the National Technical University of Athens and the Clausthal University of Technology in Germany.

First, I would like to express my sincere gratitude to my supervisor Christos Argirusis, Professor at the School of Chemical Engineering, NTUA, for granting me the opportunity to research on a current subject of which I was much interested in, in addition to his continuous support and encouragement throughout all the progress of this thesis. Next, I would like to thank Dr. Ing. Georgia Sourkouni-Argirusi from TU Clausthal for enabling the collaboration between Laboratory of Inorganic Material Science, NTUA and Clausthal Center for Materials Technology. I would also like to thank the PhD candidate Charalampia Kalogirou and the post-doctoral researchers Pavlos Pandis and Maria Savvidou, since each one contributed in their unique way to equip me with useful information needed for the experimental procedure and evaluation of the derived results. Next, I would like to thank my colleague Konstantinos Grigorakis for designing and printing the tray I had been using for the incubation of my numerous samples. Without his crucial intervention my experiments would have lasted much longer. However, foremost amongst all, I would like to express my gratefulness to Angelo Ferraro, post-doctoral Researcher at the School of Electrical and Computer Engineering, for his continuous guidance and training in liquid cultures. His ideas and opinions played a vital role in the steps that I took in the fulfillment of the present work. I would also like to thank Evangelos Christoforou, Professor at the School of Electrical and Computer Engineering, NTUA, for his cooperativeness throughout the duration of this thesis. Last but not least, I would like to thank the PhD candidate Eirini Kanellou for her assistance while performing my experiments. Finally, I would like to thank my friends and my family for their never-ending support throughout these years.

ABSTRACT

Plastics have profoundly changed what is possible in modern society. Due to their durability, low cost and resistance to degradation, coupled with low production costs, have contributed to the worldwide development of a large industry. However, their dependence on fossil fuels and their massive accumulation as waste are two main factors which have engendered a global environmental crisis. Reducing their detrimental impacts while retaining their usefulness of plastics requires a shift towards a more circular and sustainable a model of production and consumption. Biodegradation of plastics is a promising method that can be incorporated in a circular economy model. The purpose of this thesis is to study the biodegradation of poly-lactic acid (PLA), polyurethane (PU) and polycaprolactone (PCL).

After having initially outlined a theoretical background of the subject, the experimental methods and procedures are described. Pristine plastics of the three polymer types, were cut into square pieces ($10\ \mathrm{mm}$ x $10\ \mathrm{mm}$) and advanced oxidation processes (AOPs) were performed on their surface, pertaining to high and low frequency sonication ($860\ \mathrm{kH}$ and $20\ \mathrm{kH}$ respectively), UVA irradiation, combination of these techniques, as well as DBD-plasma treatment. These processes were applied to facilitate the bacteria adhesion on the surface of the samples. Samples were then placed in two diverse liquid cultures of $10\ \mathrm{mL}$, of two different strains, *Pseudomonas knackmussii* and *Pseudomonas umsongensis*. The culture medium had been renewed every two days. After the incubation, the samples were weighed, rinsed and stained with crystal violet solution in order to visualize the biofilm formed. The biofilm was then removed with the use of SDS detergent.

PLA, PU and PCL samples, independently by pretreatment methods, inoculated with *P. Umsongensis* showed a slight weight increase ($1\ \%$). Bacteria adhesion was verified; thus, biodegradation did not occur with that strain. The PLA samples that were inoculated with *P. Knackmussii* showed a slight weight decrease, with the maximum decrease being $0.64\ \%$, which is close to the error limit. PU samples incubated with *P. Knackmussii* exhibited a formation of a resilient biofilm, hence a weight increase was constantly observed. PCL samples inoculated with *P. Knackmussii* illustrated a weight decrease of $3.3\ \%$ on average in the first attempt and $0.6\ \%$ on average in the second attempt. In the third attempt, held to examine the effect of vigorous agitation on bacteria adhesion, results showed that a quantifiable weight loss was observed in plasma treated and UVA-irradiated-synergistically-sonicated samples, resulting to a weight loss of $0.83\ \%$.

The techniques performed to characterize the surface of the samples were Fourier Transform Infrared Spectroscopy (FTIR) for the observation of functional groups, Confocal Laser Scanning Microscopy (CLSM) and Optical Microscopy to scrutinize the roughness of the samples and obtain some high-resolution pictures. Moreover, a spectrophotometer was used to measure the absorbance of each flask's medium at $600\ \mathrm{nm}$, in order to estimate a bacteria growth rate. The derived IR spectra of the biodegraded samples illustrate some peaks of OH groups and nitrogen compounds that do not appear in the spectra of the neat PLA and PCL. CLSM results generally proved high roughness values.

Keywords: sonication, photodegradation, plasma treatment, bio-degradation, circular economy, PLA, PU, PCL.

Περίληψη

Τα πλαστικά υλικά έχουν αλλάξει ριζικά τη σύγχρονη ανθρώπινη δραστηριότητα. Η ανθεκτικότητά τους, το χαμηλό κόστος τους και η αντοχή στη διάβρωση, σε συνδυασμό με το χαμηλό κόστος παραγωγής, συνετέλεσαν παγκοσμίως στην ανάπτυξη μιας μεγάλης βιομηχανίας παραγωγής τους. Ωστόσο η εξάρτησή τους από μη ανανεώσιμους πόρους και η εκτεταμένη τους συσσώρευση ως απορρίμματα είναι οι δύο κύριοι παράγοντες που έχουν προκαλέσει περιβαλλοντική σε παγκόσμια κλίμακα. Η μείωση των ζημιογόνων συνεπειών τους καθώς και η διατήρηση της χρηστικότητας τους για όσο το δυνατόν μεγαλύτερο διάστημα απαιτεί την μετάβαση σε ένα πιο βιώσιμο και αειφόρο μοντέλο παραγωγής και κατανάλωσης. Η βιοαποδόμηση των πλαστικών αποτελεί μια πολλά υποσχόμενη μέθοδο η οποία δύναται να ενταχθεί σε ένα μοντέλο κυκλικής οικονομίας. Σκοπός της παρούσας διπλωματικής εργασίας είναι η μελέτη της βιοαποδόμησης του πολυγαλακτικού οξέος (PLA), της πολυουρεθάνης (PU) και της πολυκαπρολακτόνης (PCL).

Αφού αρχικά αναλυθεί το θεωρητικό υπόβαθρο του θέματος, κατόπιν περιγράφεται η πειραματική διαδικασία. Τα παρθένα πλαστικά από τα τρία παραπάνω είδη κόπηκαν σε κομμάτια διαστάσεων $10\ \mathrm{mm}$ x $10\ \mathrm{mm}$ και εφαρμόστηκαν στην επιφάνεια τους οι εξής κατεργασίες οξείδωσης: ηχο-χημικές υψηλής ($860\ \mathrm{kH}$) και χαμηλής ($20\ \mathrm{kH}$) συχνότητας, κατεργασίες φωτο-οξείδωσης (ακτινοβολία UVA), συνδυασμοί των παραπάνω, καθώς και κατεργασία με πλάσμα. Οι εν λόγω κατεργασίες εφαρμοστήκαν ώστε η επιφάνεια των πλαστικών να καταστεί πιο επιδεκτική στην μικροβιακή πρόσφυση. Ακολούθως τα δείγματα τοποθετήθηκαν σε δυο ξεχωριστές υγρές καλλιέργειες μικροοργανισμών, όγκου $10\ \mathrm{mL}$, των *Pseudomonas knackmussii* και *Pseudomonas umsongensis*. Κάθε δύο μέρες το θρεπτικό μέσο των καλλιεργειών ανανεωνόταν. Με το πέρας της βιοαποδόμησης τα δείγματα ζυγίστηκαν και έγινε χρώση τους με κρυσταλλικό ιώδες για την οπτικοποίηση του σχηματιζόμενου στην επιφάνεια βιοφίλμ. Κατόπιν το βιοφίλμ αφαιρέθηκε με τη χρήση του τασιενεργού SDS.

Τα δείγματα που εμβολιάστηκαν με τον *P. Umsongensis* παρουσίασαν μια μικρή αύξηση βάρους της τάξης του $1\ \%$, συνεπώς δημιουργήθηκε βιοφίλμ στην επιφάνεια τους, ωστόσο δεν αποδομήθηκαν. Τα δείγματα PLA που εμβολιάστηκαν με τον *P. Knackmussii* παρουσίασαν μια μικρή μείωση βάρους, με τη μέγιστη να είναι $0.64\ \%$. Ωστόσο αυτή η μείωση κρίνεται πως είναι κοντά στο όριο του σφάλματος. Στα δείγματα PU που εμβολιάστηκαν με τον *P. Knackmussii,* διμιουργήθηκε βιοφίλμ, ωστόσο σε κάθε περίπτωση παρατηρήθηκε αύξηση βάρους. Τα δείγματα PCL που εμβολιάστηκαν με τον *P. Knackmussii* παρουσίασαν μείωση βάρους $3.3\ \%$ κατά μέσο όρο στο πρώτο πείραμα και $0.6\ \%$ κατά μέσο όρο στο δεύτερο πείραμα. Στο τρίτο πείραμα με τον εν λόγω μικροοργανισμό, όπου εφαρμόστηκε ταχύτερη ανάδευση κατά την επώαση των καλλιεργειών, παρατηρήθηκε μείωση βάρους $0.83\ \%$ για το κατεργασμένο με πλάσμα και το συνδυαστικά κατεργασμένο με υπερήχους υψηλής συχνότητας και ακτινοβολία UVA δείγμα.

Οι τεχνικές που χρησιμοποιήθηκαν για το χαρακτηρισμό των επιφανειών είναι η Φασματοσκοπία Υπερύθρου (FT-IR) για την ανίχνευσή δομικών μονάδων ή δεσμών, το CLSM και η Οπτική Μικροσκοπία για την μελέτη της τραχύτητας των δειγμάτων καθώς και τη λήψη

εικόνων υψηλής ευκρίνειας της επιφάνειας των δειγμάτων. Επιπλέον έγινε χρήση φασματοφωτόμετρου για τη μέτρηση της απορρόφησης των κυττάρων στα $600\ \mathrm{nm}$ και την εκτίμηση του ρυθμού που μεγαλώνουν. Τα φάσματα Υπερύθρου των κατεργασμένων δειγμάτων εμφάνισαν νέες κορυφές που υποδεικνύουν την ύπαρξη καρβοξυλίου ή ενώσεων αζώτου και δεν εμφανίζονται στα ακατέργαστα PLA και PCL. Αυτές πιθανόν οφείλονται σε βακτηριακή ή ενζυμική δράση. Τα αποτελέσματα του CLSM έδωσαν εν γένει υψηλές τιμές τραχύτητας σε σχέση με ένα ακατέργαστο δείγμα.

Λέξεις-κλειδιά: ηχοχημεία, φωτοκατάλυση, κατεργασία πλάσματος, βιοαποδόμηση, κυκλική οικονομία, πολυγαλακτικό οξύ (PLA), πολυουρεθάνη (PU), πολυκαπρολακτόνη (PCL).

CONTENTS

LIST OF FIGURES

LIST OF TABLES

LIST OF ABBREVIATIONS

PLA	Polylactic acid
PU	Polyurethane
PCL	Poly(ε-caprolactone)
PET	Polyethylene terephthalate
AOP	Advanced Oxidation Process
US20kH	Low frequency sonication (at 20kHz)
US860kH	High frequency sonication (at 860kHz)
UV	UVA irradiation
UV+US20kH	Combinatorially UVA irradiated and low frequency sonicated
UV+US860kH	Combinatorially UVA irradiated and high frequency sonicated
ROP	ring-opening polymerization
RROP	radical ring-opening polymerization
DBD	dielectric barrier discharge

1. INTRODUCTION

1.1. Plastics Production

Plastics are high molecular weight polymers primarily synthesized from hydrocarbons and petroleum derivatives. It is estimated that about 4% of the world's fossil fuel resources are used in polymer industry [1]. Polymers also exist in nature, referring to rubber, cellulose, silk, horn, hair and DNA. The first attempt to mimic the nature was made in the 1850s by Alexander Parkes. Parkes followed not a fully synthetic procedure. He treated cellulose with nitric acid, thus creating the thermoplastic nitrocellulose, which was patented in 1862 as *Parkesine*. The following years, John Wesley Hyatt found a more viable way of producing solid nitrocellulose, which he patented in 1869 as *Celluloid*. *Celluloid* became the first commercially successful man-made polymer. But the first truly synthetic polymer was invented by Leo Baekeland who combined phenol and formaldehyde to form the *Bakelite*, patented in 1907. *Parkesine*, *Celluloid* and *Bakelite* are considered the dawn of the plastic age and nowadays are mostly of historical interest. Today, plastics comprise a large and growing number of polymers and an equally large number of additives, compounds vital for the enhancement of the final product's properties. [2]. In general, plastics are divided in two discrete categories: conventional petroleum-based polymers and bioplastics. However, the most commonly used to date are petroleum-based plastics such as polyethylene (PE), polyethylene terephthalate (PET), polyvinyl chloride (PVC), polypropylene (PP) and polystyrene (PS). *Table 1* summarizes the basic properties of these polymers and their applications.

Table 1: Commercially available plastics and their applications [3].

Plastics	Chemical Formula	Properties	Applications
PET (polyethylene terephthalate)	$(C_{10}H_8O_4)_n$	• Resistance to aging • Lightweight	• Drinking water bottles • Electronic component • Fibres in clothes
PE, HDPE (High-density polyethylene), LDPE (Low-density polyethylene)	$(C_2H_4)_n$	• Good weathering resistance • Water repellent	• Polyethylene bags • Milk carton bag lining
PVC (Polyvinyl chloride)	$(C_2H_3Cl)_n$	• Fire retarding properties • Resistance against acids, alkali and inorganic chemicals • Easily bendable with other plastics	• Health care sector • Automobiles • Building constructions and electronics
PP (Polypropylene)	$(C_3H_6)_n$	• Heat resistance and transparency	• Production of syringes, petri plates, disposable

		• High stiffness and low density	cups and plates
PS (Polystyrene)	$(C_8H_8)_n$	• Impact resistance and toughness • Poor barrier against water and oxygen • Crystal-like appearance if unfilled	• Thermal insulations • Plastic cutlery • license plate frames

There are two diverse processes of synthesizing polymers. The first, which in general corresponds to thermoplastics, involves breaking the double bond in the original olefin followed by polymerization to form new C-C bonds. Thermoplastics melt when heated. The second process, which corresponds to thermoset plastics, includes the condensation of a H_2O molecule between a carboxylic acid and an alcohol or amine to form a polyester or a polyamide. Thermosets cannot be re-melted and reformed [4].

1.2. Global production of plastics

Due to their durability, flexibility, light weight, low-cost production, bio-inertive and corrosion resistant properties, plastics dominoed an unprecedented change in the global production of goods, since their applications vary [5]. Estimations indicate that plastic production has increased worldwide from 1.5 million metric tons in 1950 to 367 million metric tons in 2020, as shown in Figure 1. At the present rate of growth, plastics production is expected to double the next 20 years. [6]

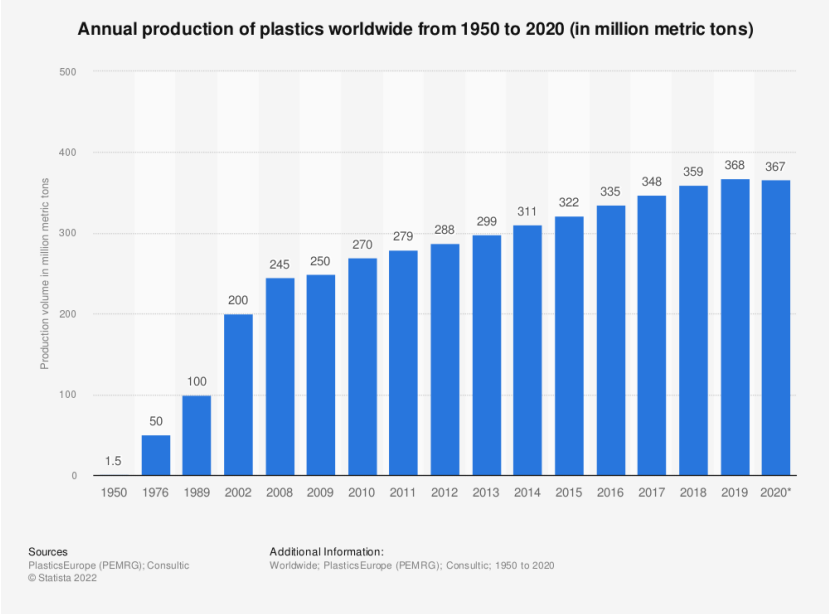

Figure 1: Production of plastics worldwide from 1950 to 2020 (in million metric tons) [6].

1.3. Bioplastics

Bioplastics are polymers that are biodegradable (can be decomposed by living organisms), bio-based (plastics synthesized from biomass or renewable resources), or can be both. More specifically, it is mainly framed in three categories of bioplastics [7]:

- Bio-based or partially bio-based and nonbiodegradable plastics like biobased Polyethylene (Bio-PE), bio-based Polyethylene terephthalate (Bio-PET)
- Bio-based biodegradable plastics, such as Polylactic acids (PLA), Polyhydroxyalkanoates (PHA), or Polybutylene succinate (PBS)
- Plastics that are based on conventional fossil resources and are also biodegradable such as Polycaprolactone (PCL).

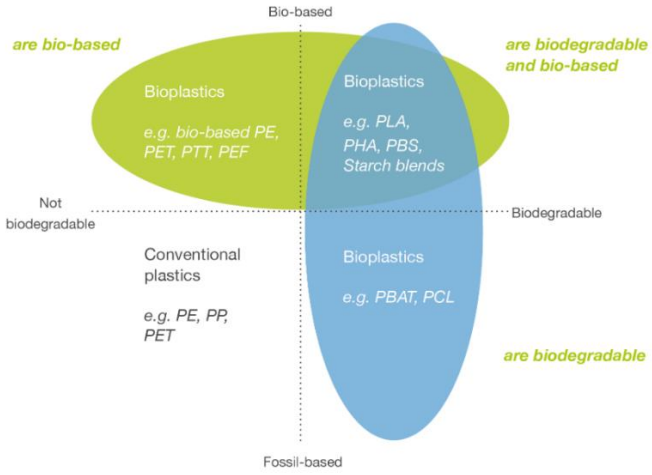

Figure 2: Biodegradable plastics, bio-plastics and their inter-relationship [8].

Bioplastics are a growing economic sector, yet only accounting a mere 1% of the total plastic production [9]. The most likely form that biodegradable plastics will take in the marketplace is by production of composites [10].

1.3.1. Poly Lactic Acid

Polylactic acid (PLA) is an aliphatic polyester that can be derived from 100% renewable resources [11]. It is a synthetic polymer based on lactic acid ($C_3H_6O_3$) and produced from the fermentation of agricultural resources, such as corn. PLA polymer is compostable, as it easily degrades by simple hydrolysis under the appropriate conditions. It was discovered in 1932 by Carothers (DuPont) who produced a low molecular weight product by heating lactic acid under vacuum. Initially, due to its high cost of manufacture, the initial uses were limited to medical and pharmaceutical applications such as controlled drug-release applications and resorbable implants. After recent advancements in the production process of the lactic acid monomer, the commercial interest in packaging and textiles applications has increased. PLA is preferred in biomedical applications due to its biodegradability, biocompatibility, and non-toxicity.

The production of PLA starts with the extraction of starch from plants such as corn or the extraction of sugar from plants such as sugar beet. If the production starts with starch, the starches are then converted to fermentable sugars (e.g., glucose and dextrose) by enzymatic

hydrolysis. Micro-organisms break the sugar into a smaller species known as lactic acid, through fermentation.

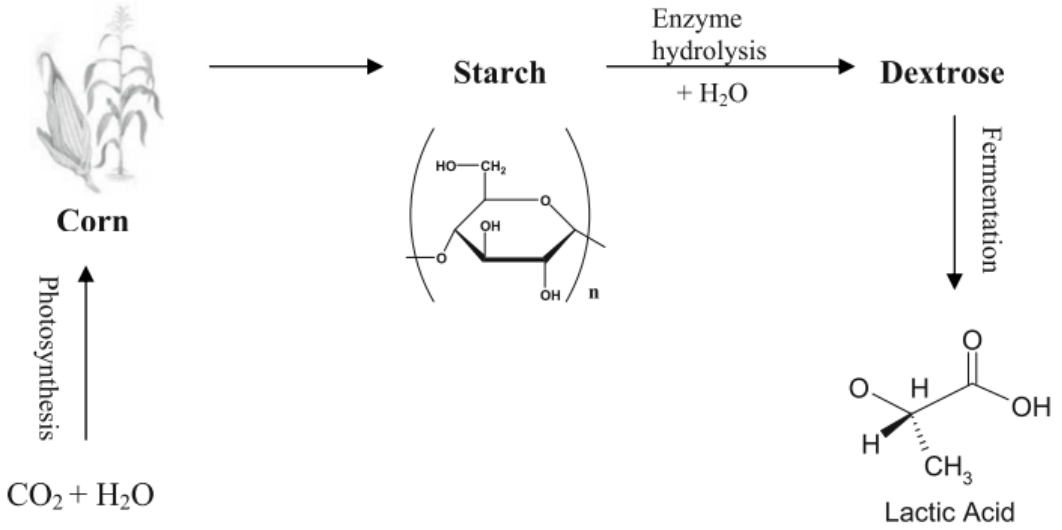

Figure 3: Production of lactic acid from renewable resources [11].

Lactic acid is the starting material for the PLA production process. There are two major routes to produce PLA from the lactic acid monomer. The conventional process for making PLA is by the polycondensation of lactic acid. This process is carried out under high vacuum and high temperature. Solvent is used to extract the water produced by the condensation reaction. Carothers used this route to produce PLA polymer. The product obtained tends to have low to intermediate molecular weight (M_w $10{,}000 - 20{,}000$) due to diffi culties of removing water and impurities.

The second method is ring-opening polymerization of a cyclic dimer of lactic acid (viz. the lactide). This method results in a higher molecular weight polymer and uses milder conditions. Production of lactide from lactic acid potentially creates three different stereoisomeric forms, namely: L-lactide, D-lactide and meso-lactide.

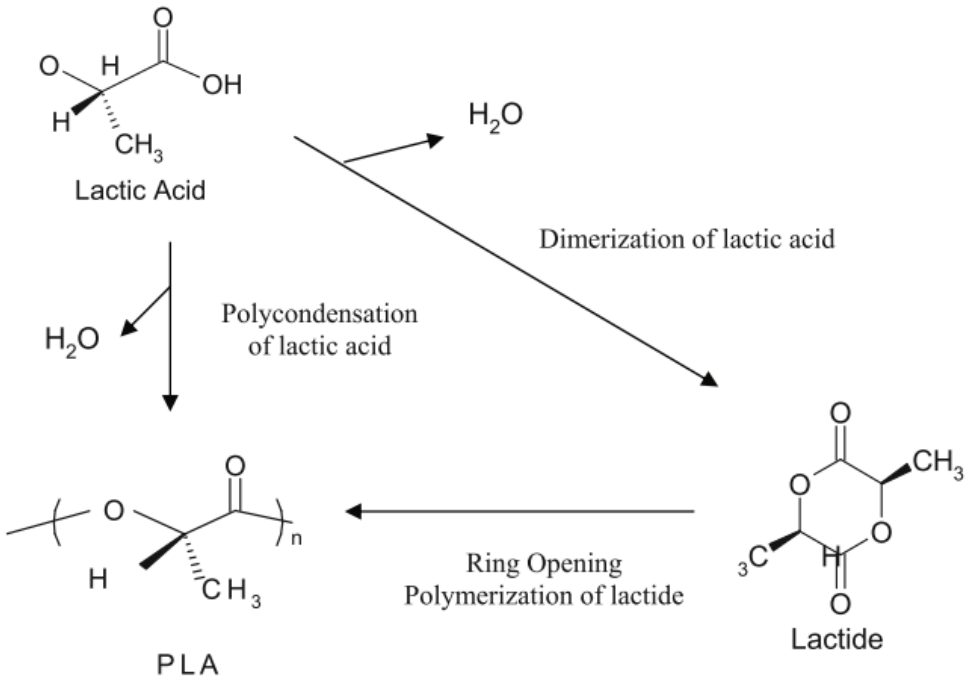

Figure 4: Polymerization routes to PLA [11].

L-lactide and D-lactide are optically active. Meso-lactide is dimerized from D- and L-lactic acids. It is optically inactive and exhibits a lower melting point than optically active lactides. Lactide is purified and ring-opening polymerization is carried out under heat without a solvent. Ring opening polymerization of lactide provides different stereopolymers depending on the isomeric type of the starting dimers. Production of PLA via the lactide route allows the possibility of modifying for superior control of the polymer properties by controlling the optical sequence of the polymer backbone. The ratio of D- and L-isomers and their distribution along the polymer backbone influence the molecular weight, crystallinity, and melting point of the end product PLA. The crystallinity of PLA decreases with increased D isomer level. Highly crystalline polymers can be achieved when the D-lactide content in the materials is less than 2%. Its glass transition temperature (T_g) is rather low, being in the range of $55 - 65℃$. PLA polymer from meso-lactide can exhibit a glass transition temperature as low as $34℃$. The melting temperature (T_m) of PLA, having either the L- or D- isomeric form alone, is between $160 - 180℃$, whereas the melting temperature of stereocomplex PLA is $220℃$. PLA exhibits good moisture management (the ability to transmit moisture away from the body with good wicking, faster moisture spreading, and drying) and comfort properties.

PLA is acknowledged to be a more environmentally-friendly polymer than PET. The monomer of PLA is sustainable. PLA, whose raw material (such as corn) is both renewable and non-polluting, eliminates the use of a finite supply of oil as a raw material. Production of PLA fibers from corn will not result in a food crisis, since the amount of corn consumed in the production of PLA fibers is less than 0.02% of the total amount of world production. Furthermore, PLA production requires $25 - 55\%$ less fossil energy and $20 - 50\%$ less fossil fuel resources than the production of petroleum-based polymers. PLA material degrades first by hydrolysis, then by microbial action (consumed by microbes), eventually degrading simply to carbon dioxide

and water, the basic necessities for new growth. The ability to recycle back to lactic acid by hydrolysis will lead to a reduction in landfill volumes [11].

1.3.2. Polycaprolactone

Polycaprolactone (PCL) is a synthetic biodegradable polyester which is produced from crude oil. It exhibits a good resistance to water, oil and chlorine [12]. PCL is a hydrophobic, semi-crystalline polymer; having a glass transition temperature (Tg) of -60℃ and melting point ranging between 59 and 64 ℃, dictated by the crystalline nature of PCL. That enables easy formability at relatively low temperatures. The number average molecular weight of PCL samples may generally vary from 3000 to $90{,}000$ g/mol and can be graded according to the molecular weight.

PCL can be synthesized by either ring-opening polymerization of cyclic monomer ε-caprolactone using a variety of anionic, cationic and co-ordination catalysts or via free radical ring-opening polymerization of 2-methylene-1- 3-dioxepane. It can also be produced by condensation of 6-hydroxycaproic acid. There are various mechanisms which affect the polymerization of PCL (anionic, cationic, co-ordination and radical), with each method affecting differently the resulting molecular weight, molecular weight distribution, end group composition and chemical structure of the copolymers [12]. Figure 6 illustrates the possible routes of synthesizing PCL either by ring opening or condensation.

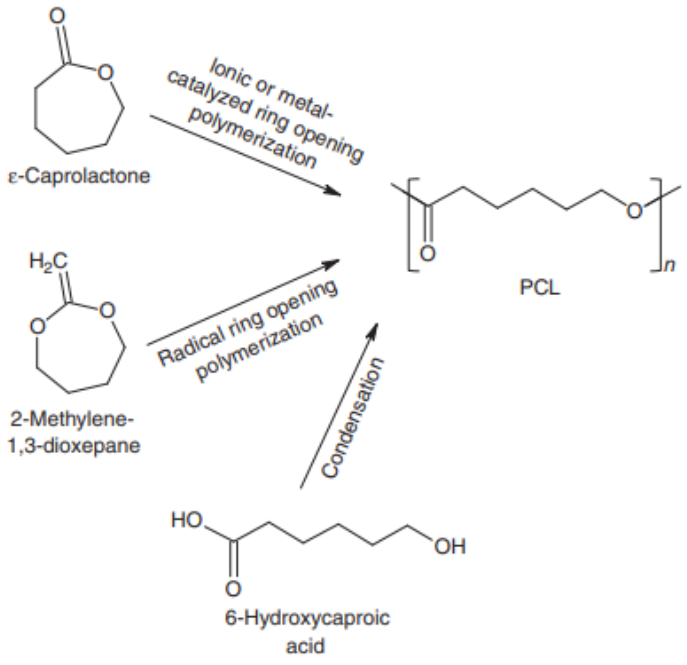

Figure 5: Synthetic routes to PCL by ionic or metal-catalyzed ROP of ε-caprolactone, by RROP of MDO and by condensation of 6-hydroxycaproic acid [13].

In general, materials based only on PCL are not used in applications where structural performances are required due to its limitations in glass transition temperature and elastic properties (Young's modulus around 0.5 GPa). Although it is a semicrystalline polymer, hence it can be used above its T_g, the elastic modulus is quite low when compared to other biodegradable polymers such as PLA [13].

PCL is suitable for controlled drug delivery due to a high permeability to many drugs and excellent biocompatibility. It also has the ability to form compatible blends with other polymers, which can affect the degradation kinetics, facilitating tailoring to fulfill its applications. Developments in tissue engineering have yielded numerous sets of tissue replacement parts such as scaffold fabrications, bone engineering, blood vessel engineering and skin engineering. Bio-nanocomposites open an opportunity for the use of new, high performance, light weight green nanocomposite materials which can replace conventional non-biodegradable petroleum-based plastic packaging materials. In food packaging, a major emphasis is on the development of high barrier properties against the diffusion of oxygen, carbon dioxide, flavor compounds and water vapor [12].

1.4. Polyurethene

Polyurethane (PU) is produced from a wide range of starting materials. Generally, PU is often synthesized by the reaction between an isocyanate and polyol molecule in the presence of either a catalyst or ultraviolet light activation. These isocyanate and polyol molecules should necessarily contain two or more isocyanate groups $(\mathrm{R}-(\mathrm{N}=\mathrm{C}=\mathrm{O})_{\mathrm{n}\geq 2})$ and hydroxyl groups $(\mathrm{R}'-(\mathrm{OH})_{\mathrm{n}\geq 2})$, respectively. Several forms in which PUs appear today are mere improvements in the invention of the German Otto Bayer and his co-workers. Figure 5 illustrates the synthesis of a typical PU [14].

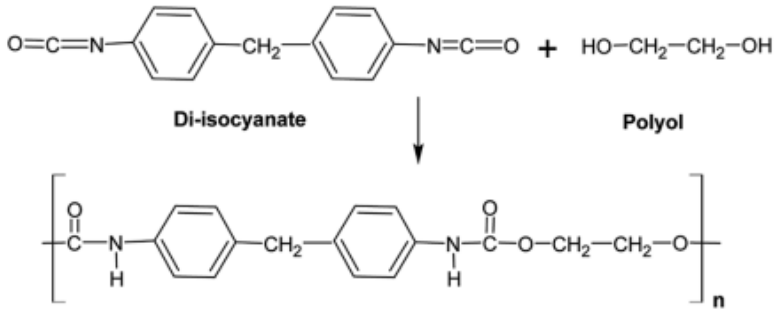

Figure 6: Synthesis reaction of the polyurethane and the most common monomers for the formation of polyurethane [14].

Table 2.The most common monomers for the formation of polyurethane.

Isocyanates	Polyols
4,4' Methylene diphenyl diisocyanate (MDI)	Polyether diol
Hexane diisocyanate (HDI)	Polyester diol
Toluene diisocyanate (TDI)	Polycarbonate diol
Isophorone diisocyanate (IPDI)	butanediol
4,4'-Methylene-bis(cyclohexylisocyanate) (HMDI)	

The exhibited properties of the PU usually depend on the types of polyols and isocyanates from which they were made. Generally, soft elastic polymers can be produced from flexible long segments of polyols ($\mathrm{M_w}$ ranging from $2{,}000$ to $10{,}000$), whereas rigid and tough polymers are obtained via a higher amount of cross-linking. Stretchy polymers can be obtained through long chains with low cross-linking, whereas hard polymers can be obtained from shorter chains with high cross-linking. On the other hand, a combination of long chains with average cross-linking would produce polymers that are suitable for foam making.

PUs may be produced through different routes, foremost amongst these being polyaddition. Other suitable additives and catalysts may also be incorporated for the PU synthesis, including include flame retardants, pigments, cross-linkers, fillers, blowing agents and surfactants. The

most common components that can be found in typical PUs and the reasons for their inclusion are presented in *Table 3*.

Table 3: Components of polyurethanes and reasons for their inclusion.

Additives	**Reasons for use**
Isocyanate	Responsible for the PU reactivity and curing properties.
Polyols	Contributes flexible long segments, which produces soft elastic polymers.
Catalysts	To speed up the reaction between the isocyanate and polyols and to allow reaction at a lower reaction temperature.
Plasticisers	To reduce material hardness
Pigments	To produce colored PU materials, especially for aesthetic purposes
Cross-linkers/chain extenders	For structural modification of the PU molecule and to offer mechanical support that will enhance the material properties.
Blowing agents/surfactants	To aid the production of PU foams, to help control the formation of bubbles during synthesis and to control the foam cell structure.
Fillers	To minimize cost and to improve the material properties, such as stiffness and tensile strength.
Flame retardants	To reduce material flammability.
Smoke retardants	To reduce the rate of possible smoke generation when the material is burnt

PUs potential applications vary. Since they exhibit an excellent heat insulation capacity, high desirable strength-to-weight ratio, versatility and durability, they can be incorporated in building and construction applications, thus facilitating the conservation of natural resources and reducing energy consumption. In the automobile industry, PUs are used for the construction of more comfortable seats, as well as in car bodies, doors, windows and ceiling sections, therefore providing better automobile mileage by reducing the car's weight. In marine and applications, PU-based epoxy resins help to protect boat hulls from corrosion and PU-based rigid foam is used to insulate boats from high temperatures and noise. Nonetheless, in medical applications PUs appear in general purpose tubing, surgical drapes, catheters, hospital bedding, wound dressing and several other injection-moulded equipment [14], [15].

1.5. Plastic pollution

The benefits that plastics brought resulted in an annual production of millions of metric tons. However, a significant portion of the produced plastics is discarded after their usage.

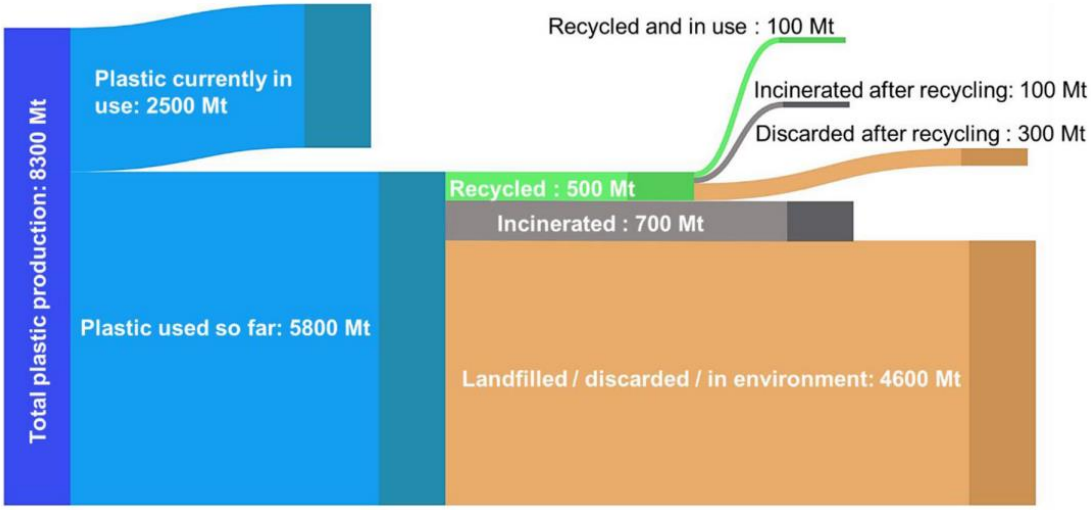

Figure 7: From the production to the discarding of plastics from 1950 to 2015 [6].

As it is shown in Figure 7, it is estimated that 8300 million metric tons of plastics have been produced between 1950 and 2015, from which only 500 million metric tons were recycled. From the plastics that are being generated as wastes, almost 9% of them are recycled. About 12% of these wastes are burned, whilst the remaining 79% of these plastics end up in the natural environment [5], [6].

Accumulation of the plastics occurs either by losses during the production processes (pre-consumer or production waste) or by direct dumping of plastic litter (post-consumer waste). As the future consumer demand for plastics increases, by year 2050 plastics manufacturing may account for as much as 20% of petroleum consumed globally and 15% of the annual carbon emissions (World Economic forum 2016). This projected increase in the production of plastics will amplify the imprint of plastic waste.

1.5.1. Classification of plastic waste found in marine and terrestrial ecosystems.

According to their size, plastic pollutants are classified as mega-debris whose size is greater than $1\ \mathrm{m}$, macro-debris whose size ranges between $20\ \mathrm{mm}$ and $1\ \mathrm{m}$ diameter, meso-debris whose size ranges between 5 and $20\ \mathrm{mm}$ and microderbis where the size is smaller than $5\ \mathrm{mm}$ [5]. Plastic particles that are much smaller ($< 1\mu\mathrm{m}$) are termed as nanoplastics. Based on the origin, microplastics are classified as primary microplastics, secondary microplastics, and nanoplastics. Primary microplastics can be defined as small-sized plastics and are presented as microplastics by design. Primary microplastics are produced directly from the consumer products like cosmetics or indirectly during the manufacture of plastics. Secondary microplastics are formed from larger plastic debris due to combined actions of chemical, physical, biological, thermal, photic, and chemical processes. Nanoplastics are tiny plastics of

sizes less than 100 nm. Nanoplastics are generated during the fragmentation and weathering of microplastic debris and can also originate from engineered material.

1.5.2. Plastic Waste Distribution

Microplastic debris are dispersed towards various, including soil, air, marine and freshwater ecosystems as well as sewage. It is indicated that there are several sources responsible for the of microplastics in soil [16], [17]. The first one is the use of plastic mulching in agricultural applications along with the input of untreated sewage wastewater for irrigation. The second one is the ingestion and digestion of plastics by earthworms, which contributes to the formation of secondary microplastics, since after this procedure plastics become brittle, thus leading to the formation of smaller fragments [16]. Furthermore, the occasional floodings of lakes and rivers contribute to the channeling of plastics to the soil. Rivers also carry large amounts of anthropogenic litter from inland sources to the ocean and coastal beaches [18]. These litter either originate from industries in the nearby areas or are disposed of by people. Regarding of the litter observed in surface seawater, plastic facilities i.e. intensive mariculture are the main source of microplastic pollution [19]. The most commonly reported microplastics are fiber-type and engineered microplastics, originating from abandoned fishing gear (nets, lines, buckets, bottles and plastic bags) with the most used resins for these applications being nylon, polypropylene and polyethylene. Likewise, rainwater facilitates the streaming of some plastic wastes from roads, construction sites and wearing tires towards treatment sewage plants. In addition, synthetic fibers are loosened from the clothes while being washed, therefore being present in municipal treatment plant sludge [20].

The increasing and uncontrolled plastic production in recent decades results in considerable pollution in the environment. The most frequently found resins in soil and marine debris are the ones used in food packaging (vacuum packs), pertaining to polyethylene, polypropylene, polyethylene terephthalate and polystyrene [17].

1.5.3. Impact on people and on environment

Microplastics have exhibited various harmful effects on humans, agriculture as well as marine and soil organisms [21]. The pollution in mariculture poses a major threat to living organisms and seafood, due to the accumulation in the food cycle. Consequently, some vital digestive tracts are blocked and the feeding behavior of a plethora of species is altered [21]. The contamination due to microplastics in agroecosystems alters the biochemical properties of the soil, due to the fact that the composition of dissolved organic matter and enzyme activity is affected. Moreover, their presence in root tips is a risk for the grazing cattle. Eventually, when humans consume products which derive from these regions, there is a fair chance of developing health problems, since the accumulated microplastics have the capability to cross biological barriers and exert toxic effects. Humans are exposed to microplastic particles via drinking water, inhalation and dermal absorption as well. The main detrimental effects are cytotoxicity and oxidative stress, while it is also reported that the microbial colonic community composition in the gastrointestinal region is altered [21], [5].

1.6. Circular Economy

According to the European Union (EU), the circular economy is a model of production and consumption, which involves sharing, leasing, reusing, repairing, refurbishing and recycling existing materials and products as long as possible, that way extending the life cycle of products as much as possible (Figure 8) [22]. In practice, it implies reducing waste to a minimum. When a product reaches the end of its life, its materials are kept within the economy wherever possible. These can be productively used again and again, thereby creating further value.

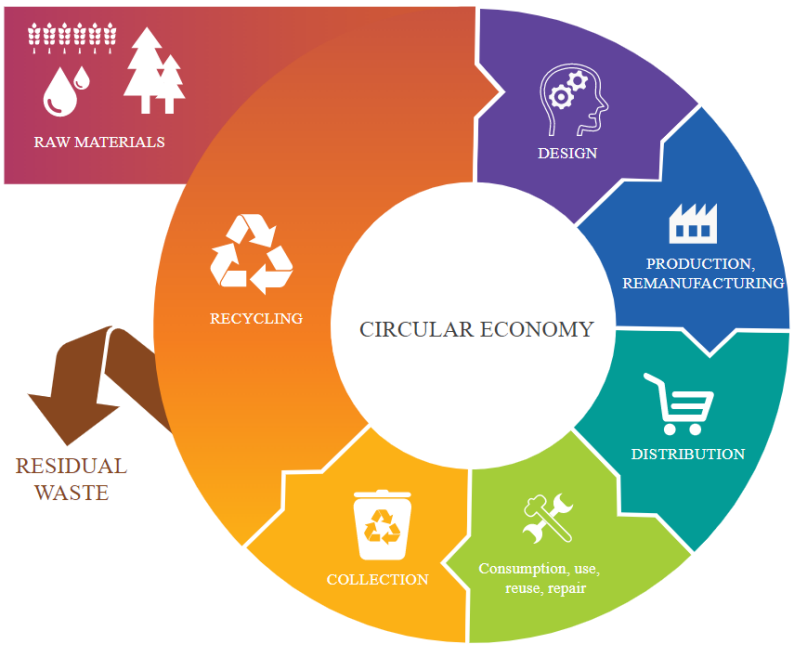

Figure 8: Schematic depiction of the circular economy model.

On the contrary, the existing linear economic model is based on a take-make-consume-throw away pattern. However, this model relies on large quantities of cheap, easily accessible materials and energy. Akin to the world's population, the demand for raw materials is growing, whilst the supplies are finite. In addition, the extended extraction and use of raw materials increases energy consumption and CO_2 emissions. More specifically, the EU produces more than 2.5 billion tons of waste every year, while the production of materials we use everyday account for 45% of the CO_2 emissions.

Moving towards a more circular economy could deliver benefits such as improving the security of the supply of raw materials while enabling developing countries be more independent. Moreover, waste prevention and eco-design will reduce pressure on the environment [22].

1.7. Biodegradation of plastics

1.7.1. Biodegradation in general

It is evident that the existing methods of limiting the plastic pollution, such as incineration and recycling are not sustainable and inefficient. Despite the fact that bioplastics have emerged as an eco-friendly solution to the plastic problem, their uncontrollable use along with a throw-away culture aggravate the existing problems. For instance, modified PLA with increased crystallinity is resistant to hydrolysis, therefore it can take over three decades to degrade in soil [10],[5]. However, it has been observed that degradation is conducted not only by moisture and radiation but by bacteria as well. There are microbes that over the years have developed the ability to digest plastic.

Biodegradation is a natural process by which organic chemicals in the environment are converted to simpler compounds, mineralised and redistributed through elemental cycles such as the carbon, nitrogen and sulphur cycles [23]. A subcategory of biodegradation is composting. Composting is a natural process by which organic material is decomposed into a soil-like substance, called humus, a soil conditioner. Decomposition is mainly performed by consortia of microorganisms (mesophilic and thermophilic), including bacteria, fungi, and actinomycetes in aerobic conditions [24].

Biodegradation is a complex process which depends on the polymer properties and the weathering conditions. More specifically, the polymer properties such as molecular weight, shape, size and additives are some main characteristics which determine biodegradability. Polymer crystallinity is also considered important, since the microbial adhesion to the polymer surface is favored in amorphous sections. Regarding to the weathering characteristics, abiotic contributors are moisture, radiation and temperature. The biotic ones are the nutrients used for the microbial growth, the extracellular enzymes which can initiate the degradation process and hydrophobicity [25]. In general, hydrophilic surfaces provide the suitable environment for the bacterial colonies to form and start digesting [26], since most of the enzymes responsible for the biodegradation are hydrophilic, except the *lipases*.

Biodegradation can be divided in two groups: microbial and enzymatic degradations. Microbial degradation is either conducted in soil, rivers and seawater, or *in vitro*, in liquid cultures and on agar plates [27], [28]. Regarding the *in vitro* microbial degradation, the plastic sample is usually inserted in the on-going culture as a whole fragment (considered as a mesodebris, size between $5 - 20$ mm). A major advantage of this method is that the enzymes responsible for degrading are continuously produced by the cells. However, this method is multivariable, therefore repetition is challenging to establish. Enzymatic degradation is held *in vitro*, usually by diluting the powdered plastic material in a desired buffer and adding a certain quantity of the enzyme to initiate the degradation. A small quantity of the enzyme should be supplemented again after a period of time. When the reaction ends the residual is removed by centrifugation, rinsed with ultra-pure water, lyophilized and weighed [29].

1.7.2. Steps of microbial biodegradation

Microbial biodegradation of polymeric materials is a multistep process that includes bio-deterioration, bio-fragmentation, mineralization and assimilation [9]. Firstly, in the bio-deterioration phase, the chemical and physical properties of the polymer are altered. In the bio-fragmentation phase, microorganisms attach to the surface of polymer substate and secrete degrading enzymes that cleave complex polymers into simpler units. In the mineralization process, short fragments of plastic get degraded and form water, methane, and carbon dioxide as the end products. In the aerobic condition, CO_2 and H_2O are formed, while under anaerobic conditions, CH_4, CO_2 and H_2O are produced. Finally, the assimilation process begins to form secondary metabolites/byproducts by integrating the atoms inside the microbial cell [30], [31].

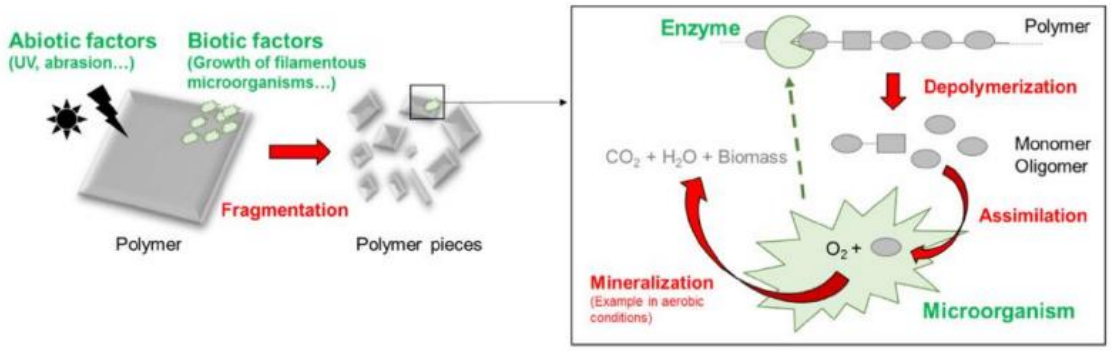

Figure 9: Polymer microbial degradation process [32].

1.7.3. The potentials of biodegradation

The existence of bacteria which excrete enzymes able to degrade either bioplastics or conventional plastics, offers an opportunity for practical waste management. A recent study of Yoshida et al. [33] introduced a two-enzyme system derived from *Ideonella Sakaiensis* which can depolymerase PET. Despite numerous reports of microbes able to degrade PET, previous work had not connected extracellular enzymatic PET degradation to catabolism in a single microbe. Yoshida et al. depicted that PETase (PET-digesting enzyme) converts PET to mono(2-hydroxyethyl) terephthalic acid (MHET), while a second enzyme, MHETase (MHET-digesting enzyme), converts MHET into the two monomers, TPA and ethylene glycol (EG).

Moreover, it has become feasible to co-cultivate two engineered microbes to accomplish both degradation and upcycling of PET simultaneously [34]. The altering of the microbes' genome is held so as to enhance the activity of the excreted enzymes. Most polymer substrates, e.g. polyurethanes, are inaccessible to enzymes, due to their insoluble hydrophobic nature. However, it has been reported that a polyurethanase from the *Comamonas acidovorans* TB-35 possesses a hydrophobic PU-surface binding domain (SBD) and a catalytic domain. This enzyme could degrade PU in a two-step reaction, with initial hydrophobic adsorption onto the PU surface via its SBD, followed by the hydrolysis of PUR ester bonds [35]. Therefore, by incorporating the responsible genes for the expression of this domain in other microbes, e.g. *E. Coli*, improvement of the degrading ability can be achieved [31].

Genetic and molecular-level analysis of genes involved in plastic degradation pathways have evolved as key factors in progressing in this field. Polymers with relatively low crystallinity are susceptible to biodegradation, whereas crystalline materials need to undergo biodegradation in higher temperatures with thermophile microbes. However, in higher temperatures the enzymes responsible for degradation are usually damaged. This obstacle can be overcome with genetic engineering, by increasing the enzyme's heat resistance [36].

1.7.4. PLA, PU and PCL biodegradation

The present dissertation focusses on the biodegradation of the synthetic polymer PU, as well as the biopolymers PLA and PCL. The production of biodegradable plastics cannot be considered a panacea to the plastic pollution, since a significant amount of them is not assimilated on the carbon cycle. A major factor that contributes to insufficient remediation of plastic waste is that blends of PLA and PCL are designed in order to improve the properties of the neat materials [14]. Thus, it is encouraging that PLA/PCL blends appear to be compostable [9]. Therefore, a rational strategy would be to initially examine under which conditions the neat polymers can be degraded by microbes. The most commonly reported microorganisms capable of digesting the examining commercial plastics are listed in *Table 4* [37], *5* [35] and *6* [38], [39], [40], [31].

Table 4: Most common PLA degrading microorganisms.

Microorganism	Representative Species	Enzyme types	Optimum temperature (°C)
Actinomycetes	*Amycolotopsis strain K104-1*	Protease	55-60
	Amycolotopsis strain 41		37-45
	Amycolotopsis strain orientalis		30
	Actinomadura strain T16-1		70
Bacteria	*Bacillus smithii* strain PL21	Esterase	60
	Alcanivorax borkumenesis ABO2449		30–37
	Rhodopseudomonas palustris RPA1511		55–60
	Paenibacillus amylolyticus strain TB-13	Lipase	50
	Alcaligenes sp.		55
	Pseudomonas tamsuii TKU015		60
Fungus	*Tritirachium album* ATCC 22563	Protease	37
	Cryptococcus sp. strain S-2	Cutinase	37

Table 5: Most common PU degrading microorganisms.

Microorganism	Enzyme types	Optimum temperature (°C)	Optimum pH
Comamonas acidovorans TB-35	Esterase	45	6.5
Pseudomonas fluorescens	Esterase	Not reported	Not reported
Pseudomonas chlororaphis	Lipase	Not reported	Not reported
Plant compost	Cutinase	70	8.0
Thermobifida fusca KW3	Cutinase	70	8.0
Thermomonospora curvata	Cutinase	60	8.5
DSM43183 Thermomonospora curvata	Cutinase	55	8.5
DSM43183 Rhodococcus equi TB-60	Urethane hydrolase	45	5.5

Table 6: Most common PCL degrading microorganisms.

Microorganism	Enzyme types	Optimum temperature (℃)
Lysunibacillus sp.70038	Not reported	30
Pseudomonas pachastrellae	Not reported	Not reported
Pseudomonas fluorescens	Lipase	37
Peudomonas cepacia	Lipase	37
Clostridium botulinum	Not reported	Not reported
Pseudomonas aeruginosa	Lipase	37

It is hypothesized that the PLA and PCL degradation follows a two-step reaction of hydrolysis conducted by serine proteases. In the first step, the active site of the serine protease binds to the surface polymer substrate. The second step involves the cleavage of peptide-like bonds present in PLA and PCL through reaction of catalytic amino acid collaborates (Ser, Asp, His) with water [41]. Degradation of PU is usually conducted by esterases, amidases, proteases and ureases with each enzyme cleaving a different bond in the macromolecule [35].

1.8. Pre – treatment methods

In order for the samples to be more susceptible to bacteria adhesion, pretreatment is necessary so as to secure a hydrophilic surface via oxidation. Moreover, the pretreatment could be conceived as a simulation to weathering (e.g. UV irradiation affects the sample as the sun radiation).

1.8.1. Sonication

Sonochemistry is a branch of research in which the molecules of a compound react chemicals, due to the application of high radiation ultrasound ($20\ \mathrm{kH}$ - $10\ \mathrm{MH}$). Ultrasonic radiation provides unusual reaction conditions (such as very high temperatures) which cannot be achieved by other methods [42].

Ultrasound irradiation of a liquid causes the formation of cavitation bubbles in it. More specific, the main event in sono-chemistry is the creation, growth, and collapse of a bubble that is formed in the liquid. Afterwards, the dissolved substance is enriched in the gaseous phase within the bubble by so called rectified diffusion leading to its growth, while the collapse of the bubble occurs when its size reaches its maximum value.

The bubbles can live several hundreds of μs and collapse upon reaching a critical radius! At this point, the collapsing bubble reaches locally (hot spot) extreme conditions with temperatures exceeding $5000\ ℃$, pressures of more than $200\ \mathrm{MPa}$ and cooling rates of up to $1010\ \mathrm{K/s}$ [42]. In those cavitations, chemical reactions are easily running often following new pathways and mechanisms [43], [44]. Such conditions have been proven favorable to nanomaterial synthesis in terms of shorter reaction times, smaller particle sizes and phase selectivity [45], [46]. Additionally, cavitations can collapse on the surface of suspended solids and the generated solvent jets modify their surface itself (mechanically) and affect its properties (surface chemistry).

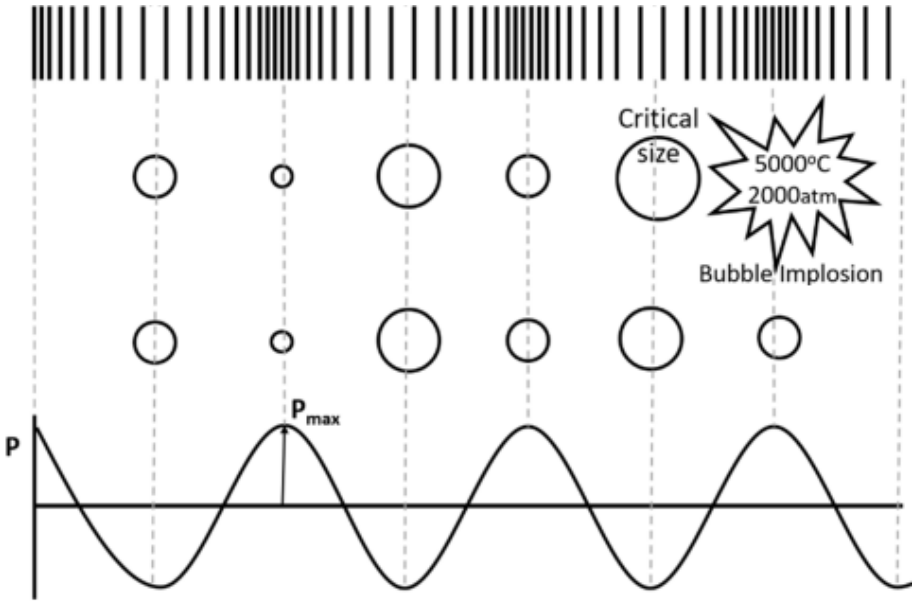

Figure 10. The principles of Sonochemistry [47].

1.8.2. Photodegradation

Photochemistry is a branch of chemistry that studies chemical effects of light. It is concerned with chemical reaction, isomerization and physical behavior that may happen due to the influence of visible and ultraviolet light [48]. UV represents a non-mechanical energy input method being able to degrade organic substances such as water-soluble pollutants but also solid organic waste such as plastics. Light can cause the decomposition of organic material and is one of the main causes of the degradation of plastic under ambient conditions.

The first law of photochemistry, often known as the Grotthuss-Draper law, described photoexcitation [49]. Photoexcitation is the initial stage of a photochemical reaction in which the reactant is raised to an excited state, which is a state with more energy. To put it in another way, the first law states that for photochemical reactions to occur, light must be absorbed by chemical compounds.

The second law of photochemistry, often known as the Stark-Einstein or photoequivalence law, states that no more than one molecule is activated for each photon of light absorbed by a chemical system in order for a photochemical reaction to occur, as specified by the quantum yield [49].

The photochemical reactions are defined by the number of photons that can activate molecules to cause the desired reaction. During a photochemical reaction, these molecules are forming a new structure. They can combine with other molecules and transfer atoms, protons, electrons, or with each other. The photochemical reaction can take place in solid, liquid, and gas phases [48].

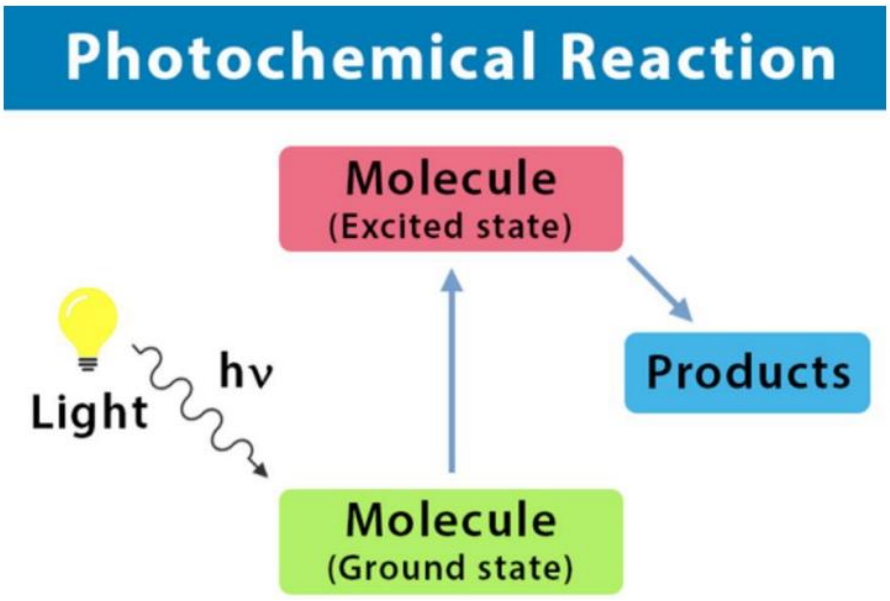

Figure 11: Principle of photochemical reaction [48].

Most synthetic polymers can be degraded by the action of ultraviolet (UVA) radiation ($400 - 290\ \mathrm{nm}$) and visible light. UVA radiation ranges between 3.1 to $4.3\ \mathrm{eV}$, which corresponds to

$72-97\ \mathrm{kcal/mol}$. This means that it has enough energy to break most chemical bonds and so light can act like thermal degradation [48].

1.8.3. Plasma Treatment

Plasma is often referred to as the fourth state of matter. The term was introduced by Langmuir in 1929, as a description of ionized gas [50]. Plasma is a partly ionized gas and can be defined as a quasi-neutral particle system in the form of gaseous or fluid-like mixtures of free electrons, ions, and radicals, generally also containing neutral particles (atoms, molecules) [51]. Some of these particles may be in an excited state and can return to their ground state by photon emission. In plasma, certain electrons are free, rather than bound to molecules or atoms. Therefore, positive and negative charges can move independently from each other. Consequently, since a very reactive environment is created while treating a surface, several different interactions between plasma and the surface are possible, pertaining to plasma polymerization, plasma treatment and plasma etching or ablation. A variety of gases is used to form a polymerized coating, create or substitute functional groups, or create radicals on the surface.

Plasmas are divided into nonequilibrium (or nonthermal/low-temperature/cold) and equilibrium (or thermal/ high-temperature/hot) plasmas. Thermal equilibrium implies that the temperature of all species (electrons, ions, neutrals, and excited species) is the same. On the contrary, plasmas with strong deviations from kinetic equilibrium have electron temperatures that are much higher than the temperature of the ions and neutrals and are classified as nonequilibrium plasmas. Plasma treating systems are used to deposit hydrophilic coatings functionalized with polar groups able per se to improve adhesion and growth of cells, but also provide chemical anchor groups for the immobilization of biomolecules (e.g., peptides, saccharides) [52]. Since high temperatures used in thermal plasmas are destructive for polymers, the majority of applications for biopolymer surface modification make use of nonthermal plasmas. Therefore, this diploma thesis introduces a cold plasma technique as a pretreatment method.

In plasma treatment, chemical functionalities are introduced onto the surfaces or free radicals are created. When the treatment takes place in ambient atmosphere, it is considered a treatment with atmospheric plasma. Ar or He typically introduces free radicals, which can react with oxygen to form (hydro)peroxides. Other plasmas, such as oxygen and nitrogen, introduce different functional groups (Figure 12) [51].

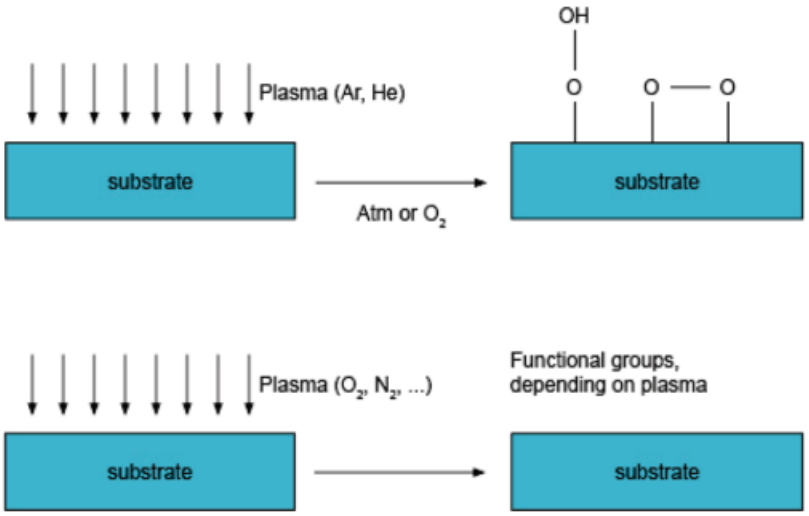

Figure 12: A schematic representation of plasma treatment with different plasma gases [51].

The simplest reactor design is the one with two parallel plates as electrodes and one or two ceramic dielectric barrier and kHz-powered sources [42].

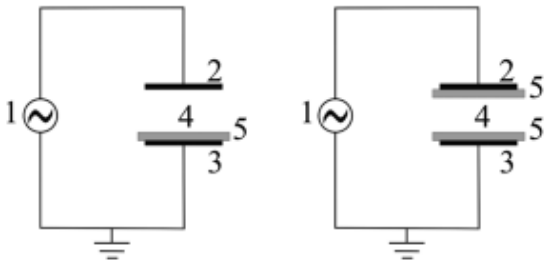

Figure 13: Typical planar DBD configuration: (1) AC HV source; (2) HV electrode; (3) ground electrode; (4) discharge gap; (5) dielectric barrier [51].

1.9. Characterization methods

1.9.1. Absorbance

Absorbance measures the capacity of a substance to absorb light of a specified wavelength. Absorbance is measured using a spectrophotometer or microplate reader, which is an instrument that generates light of a specified wavelength through a sample and measures the amount of light that the sample absorbs. In order to determine the concentration of an analyte, the wavelength at which the molecule displays the highest absorbance is utilized (peak wavelength) [53],[54].

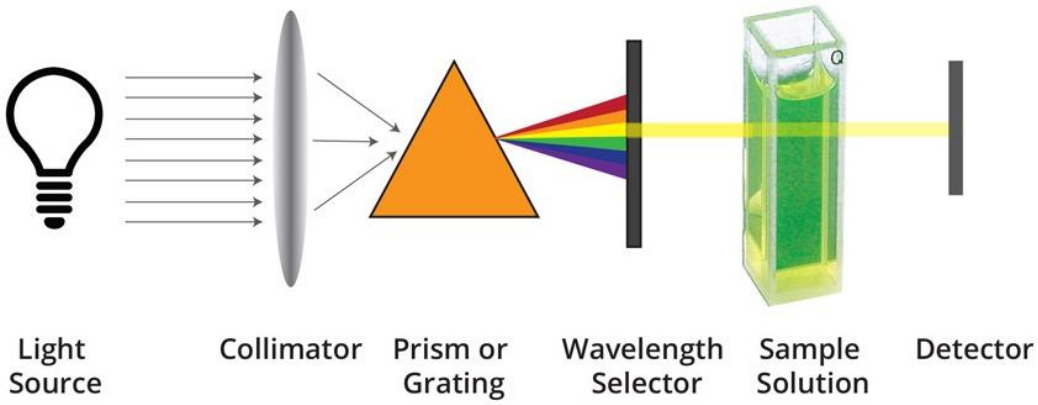

Figure 14: Simplified assembly of a photometer [53].

The Beer-Lambert law describes the relation between absorbance (A), path length (d), concentration (c) of an absorbing substance and ε, a constant that depends on the analyzed molecule (molar extinction coefficient).

$$\mathrm{A} = \mathrm{c} * \mathrm{d} * \varepsilon$$

More specifically, the Beer-Lambert law indicates that absorbance is linear to the concentration multiplied by the path length and extinction coefficient up to a certain concentration. Therefore, by measuring the absorbance of a given substance or living cells it is possible to calculate its concentration.

1.9.2. FT-IR

IR spectroscopy is a technique that uses infrared electromagnetic radiation to determine the fundamental groups that are present in molecules.

The infrared (IR) area of the electromagnetic spectrum contains radiation of wavenumbers between 12800 and $10\ \mathrm{cm}^{-1}$. This large range of radiation, is generally divided into three distinct ranges, based on the different uses of each range. The three distinct ranges of the infrared spectrum are the following [55]:

The near infrared (NIR), with wavenumbers between 12800 and $4000\ \mathrm{cm}^{-1}$.

The middle infrared (MIR), with wavenumbers between 4000 and $200\ \mathrm{cm}^{-1}$.

The far infrared (FIR), with wavenumbers between 200 and $10\ \mathrm{cm}^{-1}$.

The position of the atoms in a molecule is not fixed. Instead, the relative position of the atoms is always changing through different vibrational or rotational movements. Just as electrons can gain energy and transition to excited states, molecules can also transition to higher energy levels if they gain energy in the right amount. The bonds in molecules vibrate with a certain frequency and energy that is specific to that bond. The larger the molecule, the more the possible vibrations and interactions between atoms, which have to be taken into account [55].

There are two main types of vibrations observed in molecules: stretching and bending vibrations. When the distance between two atoms along the axis of their bond is continuously fluctuating, then the vibration is defined as a stretching vibration. There are two types of stretching vibrations: a) the asymmetrical and b) the symmetrical stretching mode. Bending vibrations are characterized by changes in the bond angle between two atoms. There are four types of bending vibrations: a) the wagging vibration, b) the rocking vibration, c) the scissoring vibration and d) the twisting vibration. The difference between these types of bending vibration is the plane where the bending occurs. Figure 15 illustrates the different types of molecular vibrations.

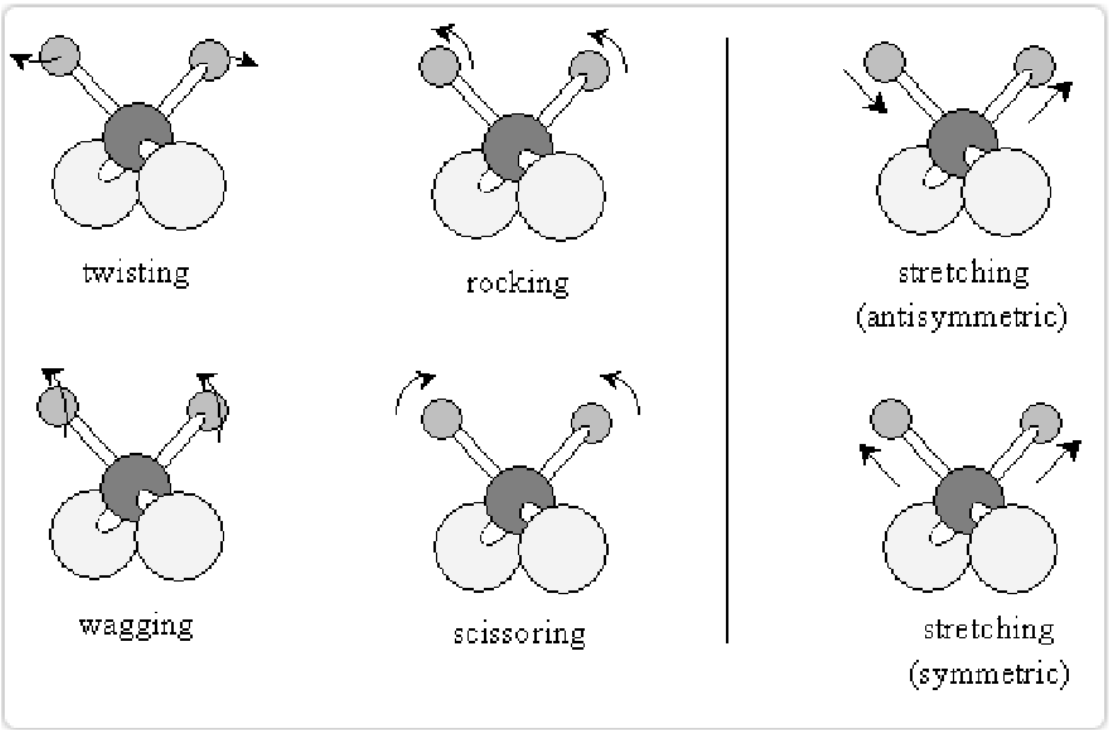

Figure 15: Types of vibration modes [56].

1.9.3. CLSM

Confocal Laser Scanning Microscopy (or CLSM) is an optical imaging technique widely used in the field of Materials Science. The principal of CLSM is quite similar to Fluorescent microscopy, however it can provide better optical resolution and observation precision by combining the

color and laser intensity information from the camera and from the laser light photoreceptor, respectively. In the case of Confocal Laser Scanning Microscopy (CLSM) a laser beam is focused on the surface of the sample. The reflected light is detected behind a pinhole aperture. This technique enables a lateral resolution that is one third better in comparison to a classic wide field microscope. By focusing the laser, the sample is scanned level by level, thus producing a three-dimensional topographic image. Here the location of maximum reflection along the beam axis is defined as a point on the surface. The intensity image produces a high-contrast microscopic image. At the same time, a classic wide field microscopic image is captured. The measurements were performed by the microscope VK-X200K from KEYENCE. The good lateral resolution (approx. $160\ \mathrm{nm}$) enables the accurate mapping of many samples. On the software side, several images can be combined to produce one large image, meaning that even when significantly enlarged, wide areas of the sample can be mapped. Because the topography of the sample is recorded, it is possible to conduct roughness analyses or profile sections. A wide field microscopic image is also captured at the same time [57].

Figure 16: the microscope VK-X200K from KEYENCE.

The important values obtained from CLSM measurements are those related to the surface roughness. The values are:

Rp, the height of the highest peak within the defined area.

Rv, the absolute value of the height of the largest pit within the defined area.

Rz, the sum of the largest peak height value and the largest pit depth value within the defined area.

Ra, as an absolute value, the difference in height of each point compared to the arithmetical mean of the surface. This parameter is used generally to evaluate surface roughness.

Rq represents the root mean square value of ordinate values within the definition area. It is equivalent to the standard deviation of heights.

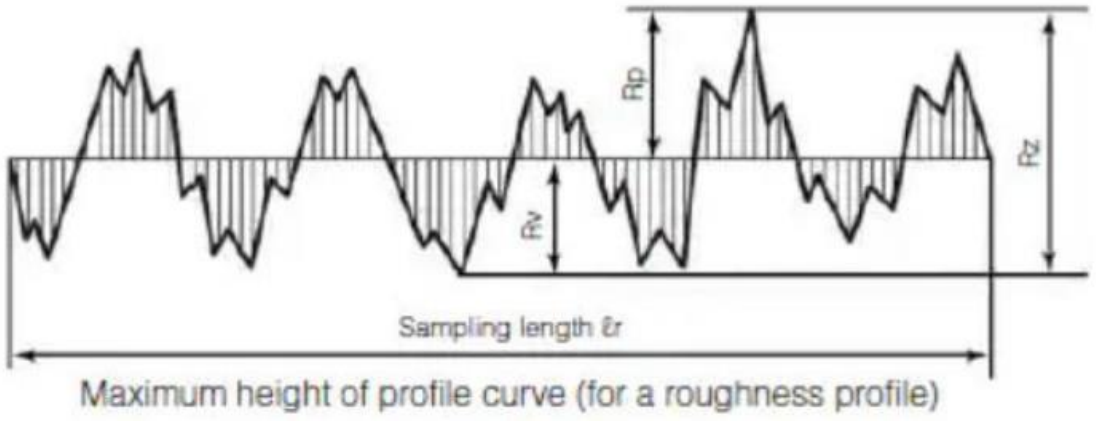

Figure 17: Representation of the values Rv, Rp, Rz.

2. EXPERIMENTAL METHODS AND PROCEDURE

2.1. PLA, PU and PCL Samples

PLA used in this study was received from Nature works, Ingeo (4043D). The % crystallinity of the pellet is 35.2 and melting point 152.3℃, melting flow ratio 6g/10min. Prior to processing the PLA pellets were dried at 50℃ for 5 hrs.

For the production of the PLA polymer film, pellets were pressed into films using a Servitech Polystat 200 T compression press at 180℃. The compression is held at 10 bar for 2 min, followed by 100 bar and 200 bar for 1 min each. The compressed sheet is crash cooled using tap water for 30 sec and demoulded.

The % crystallinity of the film was measured to be 1.9.

The pellets used for the polyurethane film production were the commercial Laripur LPR7560 Thermo plastic pellets from Coim company. The produced films illustrated an average thickness of 0.990 mm.

The pellets used for the polyurethane film production were the commercial CAPA 6500 pellets from Ravago Chemicals. The produced films illustrated an average thickness of 0.954 mm.

2.2. PRETREATMENT METHODS

2.2.1. Sonication Treatment

High-frequency ultrasound was achieved by the Ultrasound Multifrequency Generator equipped with the Ultrasound Transducer E805/T/M and an adapted glass reactor UST 02/500-03/1500 from Meinhardt® Ultrasonics, Germany, with a maximum output power of $400\ \mathrm{W/cm^2}$. The frequency was set to $860\mathrm{kHz}$ and the power amplitude to 85%.

For both low and high frequency an external Julabo recirculating cooler at $25°\mathrm{C}$ was used to help the plastics not overpass the glass transition temperature (Tg) which is low (around $55 - 60\ °\mathrm{C}$) and also protect the high-frequency equipment, which may be damaged at temperatures above $50\ °\mathrm{C}$. Temperature was controlled at $25\ °\mathrm{C}$ for the pretreatments of $860\ \mathrm{kHz}$ and $20\ \mathrm{kHz}$.

Figure 18: Sonication treatment

2.2.2. UV Treatment

The samples were immersed in deionized water in a UVA transparent beaker and put on a stirring plate in the home-made UV reactor. The reactor has three $11\ \mathrm{W}$ UVA lamps on each side and thus the samples were exposed to $66\ \mathrm{W}$ UVA irradiation under continuous stirring. No photocatalytic active materials were used in the UV experiments.

2.2.3. Combination of UVA Irradiation and Ultrasounds

In addition, the plastics were treated with UVA irradiation and Ultrasounds at the same time in order to observe whether this combinatorial technique has a better effect on their surface. More specifically, the reactor illustrated in Figure 19 was transferred in the UV reactor, for the execution of two diverse combinatorial techniques:

- low frequency sonication ($20\mathrm{kH}$) combined with UV treatment
- high frequency sonication ($860\mathrm{kH}$) combined with UV treatment

Figure 19. Combination of UV treatment and high frequency sonication – experimental setup.

2.2.4. DBD Plasma Treatment

The samples were put in a self-made parallel plate dielectric barrier discharge (DBD) reactor in order to be treated with an atmospheric DBD plasma at ambient air. The DBD is made from the ceramic Al_2O_3. The DBD plasma conditions were $16\ \mathrm{kV}$ at a frequency of $7\ \mathrm{kHz}$ and the distance between the electrodes was set to $3\ \mathrm{mm}$. Both sides of the samples were treated for $20\ \mathrm{sec}$.

Figure 20: DBD plasma reactor – sample placement.

Figure 21: DBD plasma reactor in operation.

2.3. BIODEGRADATION

Two different strains were selected to test their potential ability to digest the aforementioned diversities of plastics: *Pseudomonas knackmussii* B13 and *Pseudomonas umsongensis* GO16. Comparative genomic analysis showed that the former is phylogenetically close to *Pseudomonas aeruginosa* species that is known to have the ability to cleave long chain alkanes [58]. *Pseudomonas Umsongensis* is a versatile strain with the potential to upcycle the residuals of degradation of some polymers, such as PET, to form PHAs [59].

Biodegradation:

For the cultivation of the strain *Pseudomonas knackmussii* the following media are prepared.

Table 7: Components and quantities for the preparation of the Mineral Medium (CM).

Mineral Medium (Complementary Medium=CM)
1.22 g Na_2HPO_4
0.76 g KH_2PO_4
0.25 g $(NH_4)_2SO_4$
0.10 g $MgSO_4$ x 7 H_2O
0.025 g $CaCl_2$ x 2 H_2O
5 mL SL4
500 mL Distilled water
Adjust pH to **6.9**

Table 8: Components and quantities for the preparation of the Trace Element Solution SL6.

Trace Element Solution SL6
0.0100 g $ZnSO_4$ x 7 H_2O
0.0030 g $MnCl_2$ x 4 H_2O
0.0300 g H_3BO_3
0.0200 g $CoCl_2$ x 6 H_2O
0.0010 g $CuCl_2$ x 2 H_2O
0.0020 g $NiCl_2$ x 6 H_2O
0.0030 g Na_2MoO_4 x 2 H_2O
100 mL Distilled water

Table 9: Components and quantities for the preparation of the Trace Element Solution SL4.

Trace Element Solution SL4
0.125 g EDTA
0.05 g $FeSO_4$ x 7 H_2O
25 mL Trace Element Solution SL6
225 mL Distilled water

Table 10: Components and quantities for the preparation of the Peptone & Meat extract medium (PM).

Peptone & Meat extract (PM)
2.5 g Peptone
1.5 g Meat Extract
500 mL Distilled water
Adjust pH to **7**

For the strain *Pseudomonas umsongensis* the following media are prepared.

Table 11: Components and quantities for the preparation of the Trace Element Solution.

Trace Element Solution
0.5 g $MnCl_2 \cdot 4H_2O$
2 g $ZnSO_4 \cdot 7H_2O$
0.15 g $NiCl_2 \cdot 6H_2O$
0.5 g $Na_2MoO_4 \cdot 2H_2O$
0.5 g $CuCl \cdot 2H_2O$
3.8 g $FeSO_4 \cdot 7H_2O$
500mL Distilled water
Adjust **pH** to **7**

Table 12: Components and quantities for the preparation of the Peptone & Meat extract medium (PM').

Peptone & Meat extract + NaCl (PM')
2.5 g Peptone
1.5 g Meat Extract
1.5 g NaCl
500 mL Distilled water
Adjust pH to **7**

CM an PM media are autoclaved ($121℃, 20$ min) (Figure 22) and stored at room temperature. The trace element solutions are filtrated and stored in the refrigerator.

Figure 22: Autoclave.

Revitalization and cultivation of the strain *Pseudomonas knackmussii*:

In order to revitalize the strain *Pseudomonas knackmussii*, the pellet which includes the freeze-dried cells is diluted in $10\ \mathrm{mL}$ of cultivation medium (40% PM, 60% CM) and incubated at $30℃$ overnight ($160\mathrm{rpm}$). The following day, $1\mathrm{mL}$ of the grown cells is diluted with $250\mathrm{mL}$ of cultivation medium. This expansion of the volume is required for the cells to grow properly. All the aforementioned culture media are prepared in the laminar flow cabinet to guarantee sterility (Figure 23).

For the revitalization of the strain *Pseudomonas umsongensis*, the same procedure is followed by producing a cultivation medium with 40% PM' and 60% distilled water.

Figure 23: Laminar flow cabinet.

Glycerol Stocks:

The following day, $8\ \mathrm{mL}$ of the cells are diluted with $2\mathrm{mL}$ of glycerol (Figure 24). 10 glycerol stocks of $1\mathrm{mL}$ are produced and stored at $-20℃$ for eventual future use.

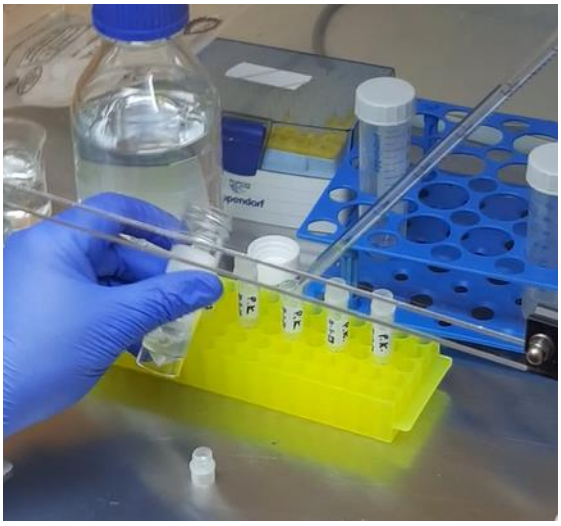

Figure 24: Glycerol stocks.

Starvation of the strain and biodegradation:

The medium for the starvation of the strain *Pseudomonas knackmussii* is prepared ($20\ \%$ PM, $80\ \%$ CM). The Blank sample is put in a falcon with $10\ \mathrm{mL}$ of the prepared medium. In an Erlenmeyer flask, the required quantity of the starvation medium is diluted with $1-2\ \%$ of grown cells. Each sample is weighed using an OHAUS Adventurer™ Analytical balance and put in a marked falcon. $10\ \mathrm{mL}$ of the produced medium is delivered with a pipet to each falcon. All falcons are placed in a custom-made falcon tray and incubated for 3 weeks ($120\ \mathrm{rpm}, 30℃$) (Figure 25). Every two days $5\ \mathrm{mL}$ of culture are removed from the falcon which contains the pretreated samples and replaced with $5\ \mathrm{mL}$ of fresh medium. After three weeks the samples are removed.

For the starvation of the strain *Pseudomonas umsongensis* a medium containing 20% PM, 75% distilled water and 5% trace element solution is prepared.

Figure 25: Biodegradation of the plastic samples: Incubation.

Visualization of the biofilm:

The reference sample is rinsed with water, ethanol and weighed. The pretreated samples are rinsed with ethanol and let to dry. Afterwards they are dipped into crystal violet solution (1 g of crystal violet powder, 50 mL of ethanol, and the total volume is adjusted to 1 L with distilled water). Then they are rinsed with 80% acetic acid, let to dry, and weighed. It can be stated that a biofilm has been formed, if the sample is violet (Figures 26 and 27).

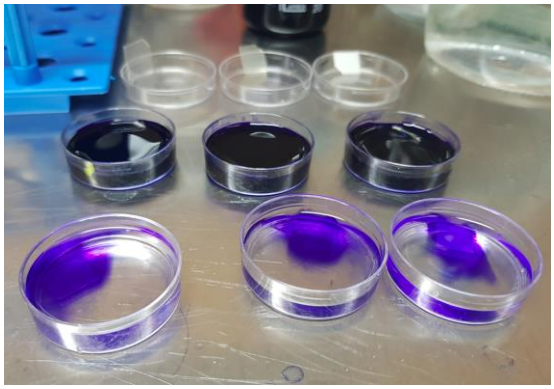

Figure 26: Samples stained with 80% acetic acid.

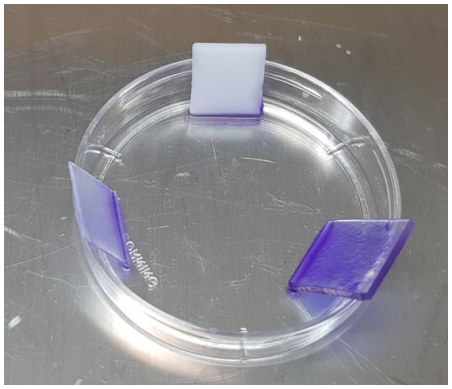

Figure 27: Samples after staining with acetic acid.

Removing the Biofilm:

The biofilm is removed with SDS detergent (2% SDS powder). Then the sample is weighed again.

Four different experiments were performed:

1st Experiment: 3 weeks of biodegradation using the strain *Pseudomonas knackmussii* (30°C, 120 rpm). For each pretreatment method and each type of plastic, three samples are

incubated, each one corresponding to a whole week of biodegradation. After the incubation, the samples were dipped in crystal violet solution, rinsed with 80% acetic acid and weighed.

2nd Experiment: 3 weeks of biodegradation using the strain *Pseudomonas umsongensis* (30℃, 120 rpm). The samples underwent the same treatment as in the 1st Experiment.

3rd Experiment: 6 weeks of biodegradation using the strain *Pseudomonas knackmussii* (30℃, 120 rpm). When the third week of incubation was completed, samples were weighed and dipped in 2% SDS solution in order for the biofilm to be removed. Afterwards they were weighed again and incubated for another 3 weeks.

4th Experiment: 6 weeks of biodegradation using the strain *Pseudomonas knackmussii* (30℃, 250 rpm). After the incubation, the samples were dipped in crystal violet solution, rinsed with 80% acetic acid and weighed. Then they were dipped in 2% SDS solution in order for the biofilm to be removed. Afterwards they were weighed again.

Note: These experiments were conducted once, due to restricted available time. To establish more valid results, biodegradation experiments are usually conducted in triplicate.

Absorbance Measurement

Every two days, 2 mL of medium were removed from each flask and transferred to cuvettes. The absorption measurement at 600 nm is used to calculate the increase of bacteria [60]. The absorbance at 600 nm was measured using a spectrophotometer in order to calculate the growth ratio. The same measurement was performed for cells which grow without any plastic sample in their falcon, in order to compare the growth ratios.

Optical Microscope

All samples were examined under an optical microscope (Examet Union). Screenshots of 10x were obtained.

3. RESULTS

3.1. Mass Variation & Optical Density

1st Experiment

After having weighed every sample each week, the results of biodegradation using the strain *Pseudomonas knackmussii* are depicted in Figures 28, 29, 30 and 31. The PLA and PCL Blank samples maintained their weight and the flasks contained a transparent solution. However, the flask of the PU Blank sample was contaminated probably by the sample itself due to deficient sterilization. It is important to note that the diagrams constructed using results of the 1st and the 2nd experiment should have better been presented as dots (symbols), rather than dots and lines, since every week's symbol corresponds to a different sample. However, lines were used to make each pretreatment method distinguishable.

PLA and PU samples:

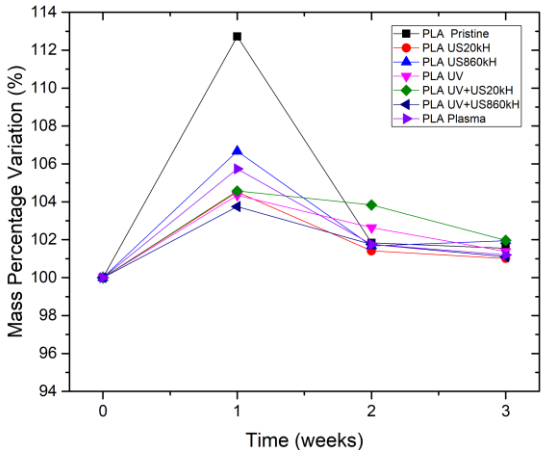

Figure 28: Mass of each PLA sample throughout 3 weeks of biodegradation.

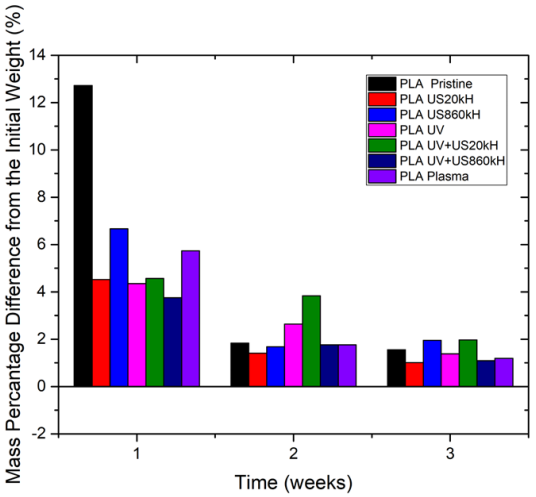

Figure 29: Mass variation of each PLA sample after 3 weeks of biodegradation.

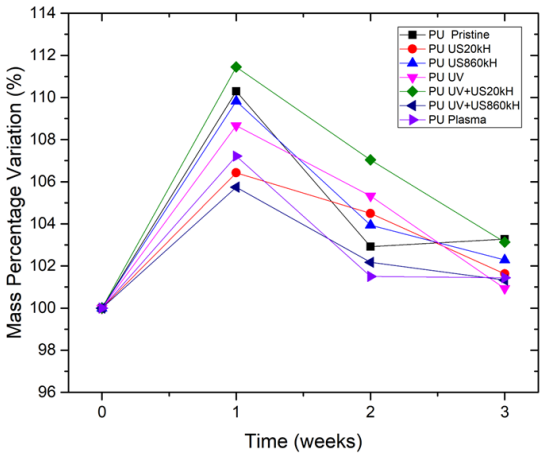

Figure 30: Mass of each PU sample throughout 3 weeks of biodegradation.

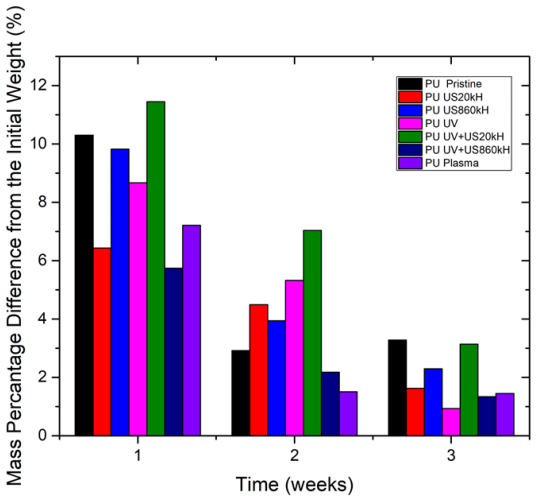

Figure 31: Mass variation of each PU sample after 3 weeks of biodegradation.

The PLA and PU samples illustrate a weight increase the first week, 6.05% and 8.5% on average, respectively, due to the formation of the biofilm. From that point on, either biodegradation takes place, or the bacteria remain attached on the samples without degrading them.

Theoretically, if the growth ratio of the bacteria that grow with the plastic is greater than those growing without plastic, it implies that the strain digests the polymer. If the reference possesses a greater growth ratio, it is still possible that the bacteria digest plastic but they prefer peptone as a primary source of carbon. Considering the results of the absorbance measurements, the growth rate of the bacteria did not give any insight into which pretreatment methods are the most favorable for bacteria adhesion. Indicatively, the third week, the growth ratio of the bacteria that grow with plastic was either almost equal or less that the growth ratio of the bacteria that grow with plastic.

Table 13: The growth ratio of the strain P. Knackmussii cultivated with PLA the 3rd week of biodegradation

Samples	Initial Absorbance	Final Absorbance	Growth Ratio	Normalized Growth Ratio
Reference (no plastic)	0.480	0.856	1.783	1.000
PLA Pristine	0.521	0.758	1.455	0.816
PLA US20kH	0.417	0.739	1.772	0.994
PLA US860kH	0.423	0.765	1.809	1.014
PLA UV	0.450	0.719	1.598	0.896
PLA US20kH+UV	0.433	0.753	1.739	0.975
PLA US860kH+UV	0.386	0.750	1.943	1.090
PLA Plasma	0.431	0.791	1.835	1.029

Table 14: The growth ratio of the strain P. Knackmussii cultivated with PU the 3rd week of biodegradation.

Samples	Initial Absorbance	Final Absorbance	Growth Ratio	Normalized Growth Ratio
Reference (no plastic)	0.480	0.856	1.783	1.000
PU Pristine	0.346	0.682	1.971	1.105
PU US20kH	0.360	0.624	1.733	0.972
PU US860kH	0.391	0.751	1.921	1.077
PU UV	0.427	0.707	1.656	0.928
PU US20kH+UV	0.364	0.648	1.780	0.998
PU US860kH+UV	0.461	0.754	1.636	0.917
PU Plasma	0.419	0.842	2.010	1.127

The PCL samples illustrate a significant weight decrease of 3.2 % on average the first week, except the plasma treated sample, whose weight directly increases (Figures 32, 33).

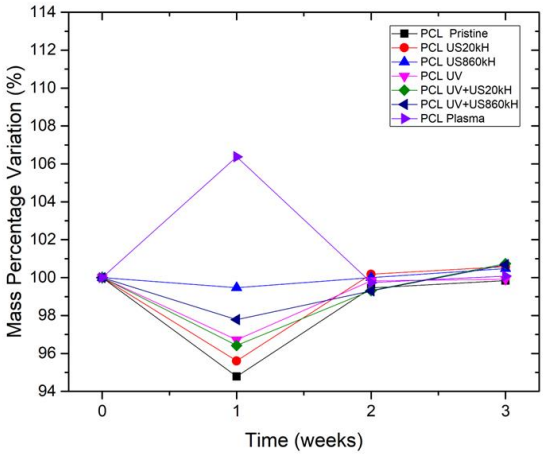

Figure 32: Mass of each PCL sample throughout 3 weeks of biodegradation.

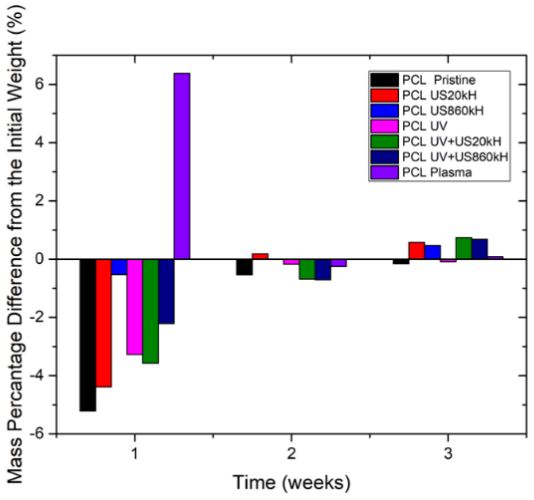

Figure 33: Mass variation of each PCL sample after 3 weeks of biodegradation.

This could be mainly because the plasma-treated sample possesses many free groups which favor the immediate interaction with bacteria. The pristine sample of the first week showed an unexpected weight decrease of 5.2 %, while the pretreated samples with the most promising results were the low frequency sonicated, the UV irradiated and the samples treated simultaneously by both AOPs. A probable explanation for the first week's sudden weight decrease could be that bacteria started damaging the surface of the plastic to create free radicals. Once the radicals were created, bacteria extended their colonies and stopped digesting the plastic, most likely due to contamination.

The results of the absorbance measurements indicate an analogous inconsistency to the growth ratios expected. The media of the samples which exhibited the sharpest weight decrease were expected to have a normalized growth ratio greater than 1. This is another evidence of contamination of some flasks the third week.

Table 15: The growth ratio of the strain P. Knackmussii cultivated with PCL the 3rd week of biodegradation.

Samples	Initial Absorbance	Final Absorbance	Growth Ratio	Normalized Growth Ratio
Reference (no plastic)	0.480	0.856	1.783	1.000
PCL Pristine	0.422	0.738	1.749	0.981
PCL US20kH	0.391	0.778	1.990	1.116
PCL US860kH	0.453	0.752	1.660	0.931
PCL UV	0.483	0.748	1.549	0.868
PCL US20kH+UV	0.458	0.852	1.860	1.043
PCL US860kH+UV	0.373	0.762	2.043	1.146
PCL Plasma	0.441	0.808	1.832	1.027

Despite the aforementioned inconsistencies, these results seem very promising, considering the first week's weight loss. Eventual repetition would establish a more certain statement as to whether these results are valid.

2nd Experiment

In the 2nd experiment, the recorded weights for PLA, PU and PCL samples were less promising (Figures 34, 35, 36, 37, 38 and 39).

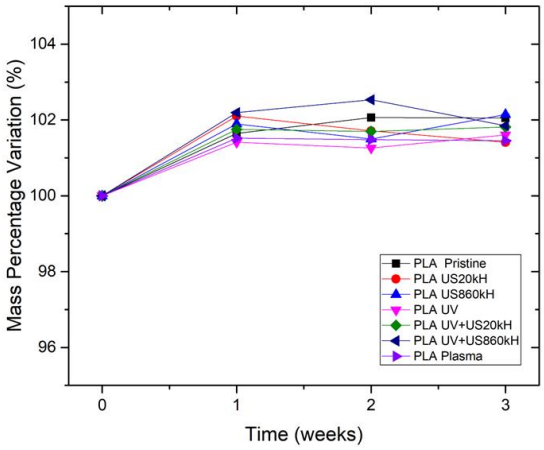

Figure 34: Mass of each PLA sample throughout 3 weeks of biodegradation.

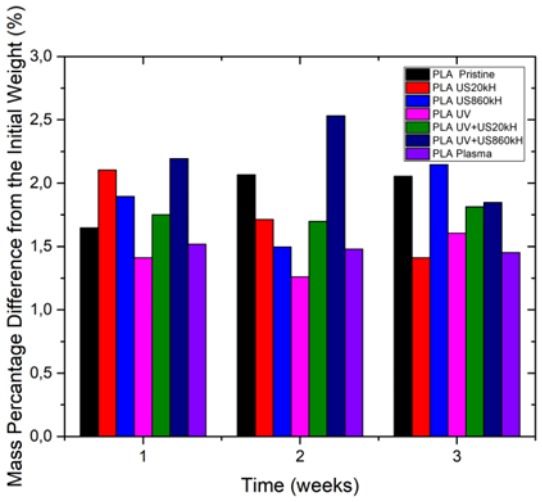

Figure 35: Mass variation of each PLA sample after 3 weeks of biodegradation.

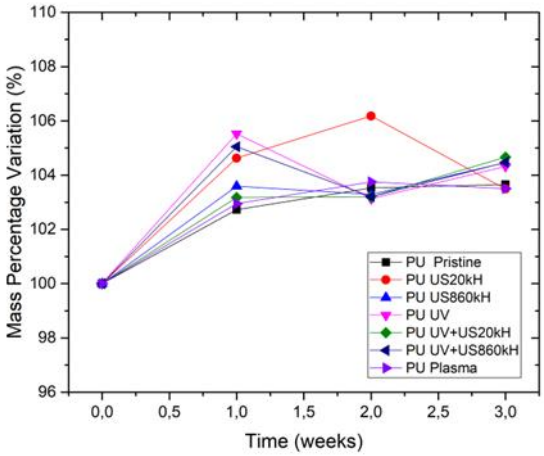

Figure 36: Mass of each PU sample throughout 3 weeks of biodegradation

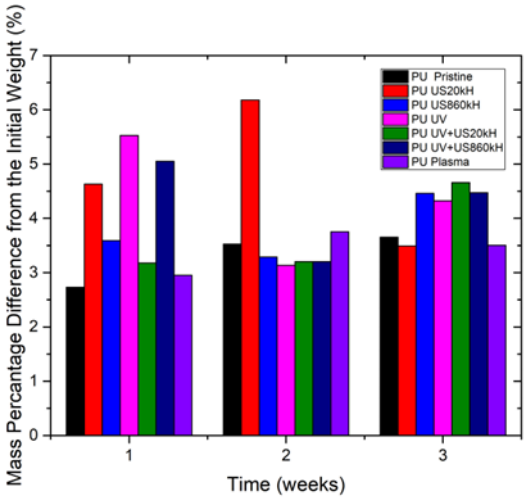

Figure 37: Mass variation of each PU sample after 3 weeks of biodegradation.

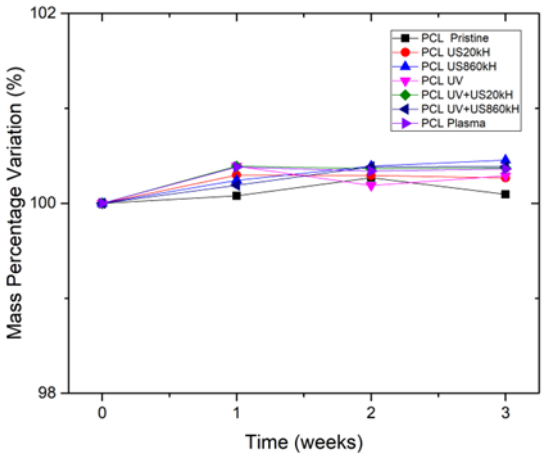

Figure 38: Mass of each PCL sample throughout 3 weeks of biodegradation

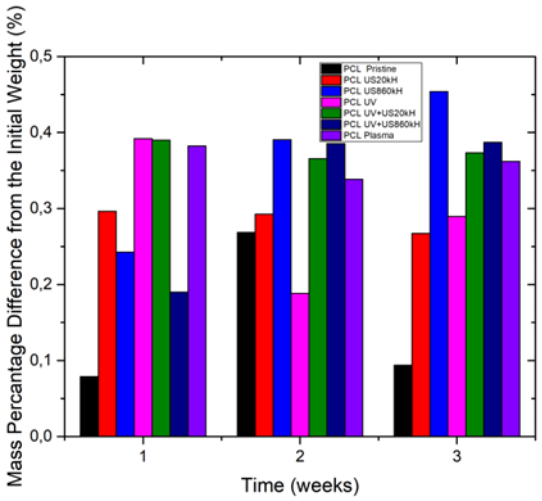

Figure 39: Mass variation of each PCL sample after three weeks of biodegradation.

In all three types of plastics an insignificant weight increase of about 1 % was observed and the formation of a tiny biofilm was verified with the crystal violet method. The growth ratios of the third week indicate that the cells grew a lot despite the fact that they did not degrade the plastic. Therefore, either contamination has occurred, or bacteria need to be starved in a lower concentration of peptone so as to be forced to digest.

Table 16: The growth ratio of the P. Umsongensis cultivated with PLA the 3rd week of biodegradation.

Samples	Initial Absorbance	Final Absorbance	Growth Ratio	Normalized Growth Ratio
Reference (no plastic)	0.222	0.346	1.559	1.000
PLA Pristine	0.250	0.494	1.976	1.268
PLA US20kH	0.196	0.411	2.097	1.345
PLA US860kH	0.192	0.352	1.833	1.176
PLA UV	0.236	0.435	1.843	1.183
PLA US20kH+UV	0.208	0.365	1.755	1.126
PLA US860kH+UV	0.209	0.368	1.761	1.130
PLA Plasma	0.206	0.354	1.718	1.103

Table 17: The growth ratio of the P. Umsongensis cultivated with PU the 3rd week of biodegradation.

Samples	Initial Absorbance	Final Absorbance	Growth Ratio	Normalized Growth Ratio
Reference (no plastic)	0.222	0.346	1.559	1.000
PU Pristine	0.264	0.529	2.004	1.286
PU US20kH	0.190	0.395	2.079	1.334
PU US860kH	0.231	0.441	1.909	1.225
PU UV	0.213	0.382	1.793	1.151
PU US20kH+UV	0.224	0.425	1.897	1.217
PU US860kH+UV	0.195	0.347	1.779	1.142
PU Plasma	0.219	0.347	1.584	1.017

Table 18: The growth ratio of the P. Umsongensis cultivated with PCL the 3rd week of biodegradation.

Samples	Initial Absorbance	Final Absorbance	Growth Ratio	Normalized Growth Ratio
Reference (no plastic)	0.222	0.346	1.559	1.000
PCL Pristine	0.253	0.527	2.083	1.336
PCL US20kH	0.193	0.409	2.119	1.360
PCL US860kH	0.220	0.403	1.832	1.175
PCL UV	0.218	0.416	1.908	1.224
PCL US20kH+UV	0.202	0.389	1.926	1.236
PCL US860kH+UV	0.217	0.367	1.691	1.085
PCL Plasma	0.206	0.354	1.718	1.103

3rd Experiment

As it has been observed in the previous experiments, during the first week of biodegradation a biofilm is formed. The main goal of this experiment is to examine what happens after removing the biofilm, by extending the time of incubation for another 3 weeks.

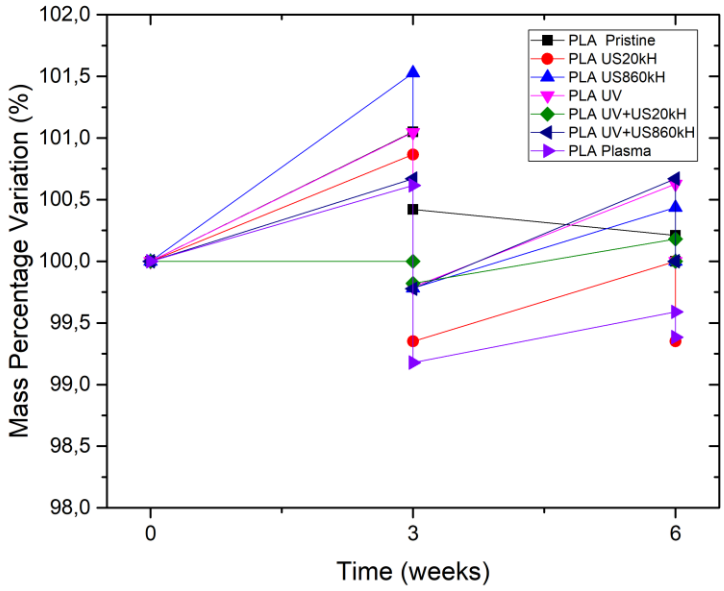

Figure 40: Mass of each PLA sample throughout 6 weeks of biodegradation.

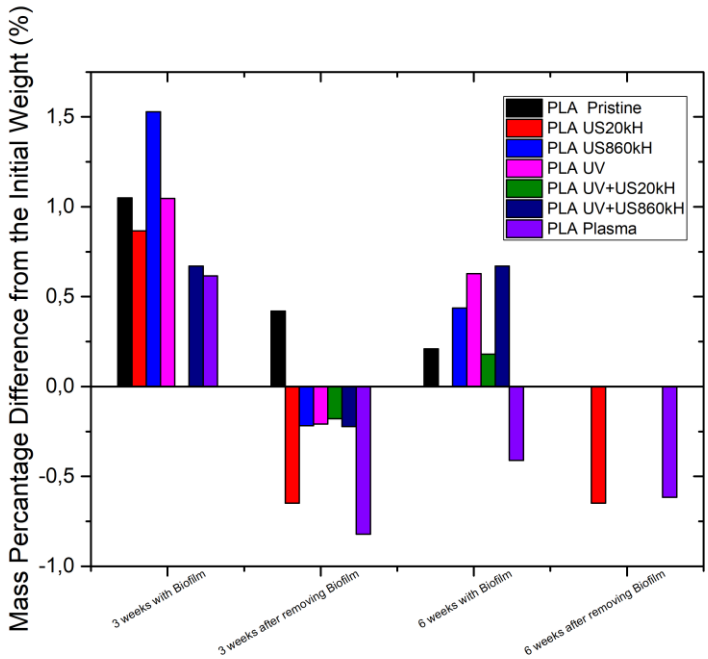

Figure 41: Mass variation of each PLA sample after 6 weeks of biodegradation

Figures 40 and 41 illustrate that every PLA sample, (except the UV+US20kH sample) has experienced a weight increase after every incubation. After the first three weeks, the biofilm was removed and the weight of every sample was less than the initial. Hence, the next three weeks of biodegradation a new biofilm was formed, but after removing it, only low frequency sonicated and plasma treated samples gave result that may indicate potential degradation. However, these weight losses are considered negligible since they are close to the balance error limit. Indicatively, the initial weight of the plasma treated sample was 0.0487 g and after 6 weeks the final weight, having removed the biofilm, was 0.0484 g. That corresponds to 0.62% weight loss.

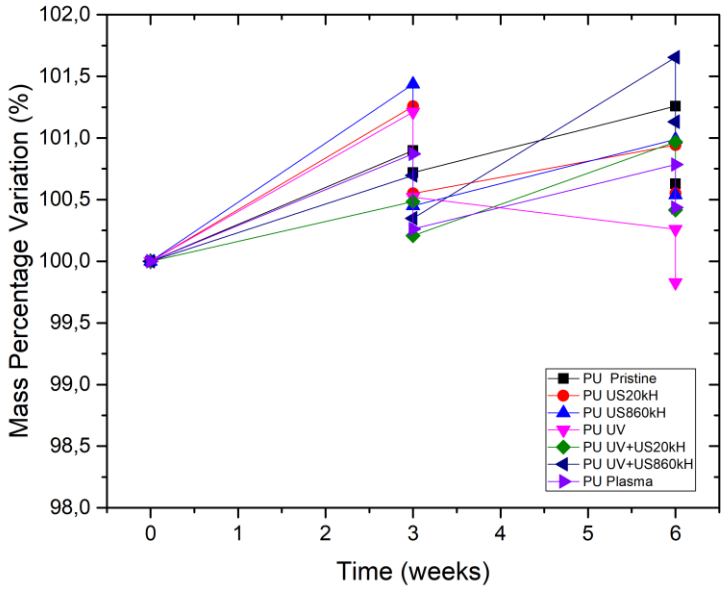

Figure 42: Mass of each PU sample throughout 6 weeks of biodegradation

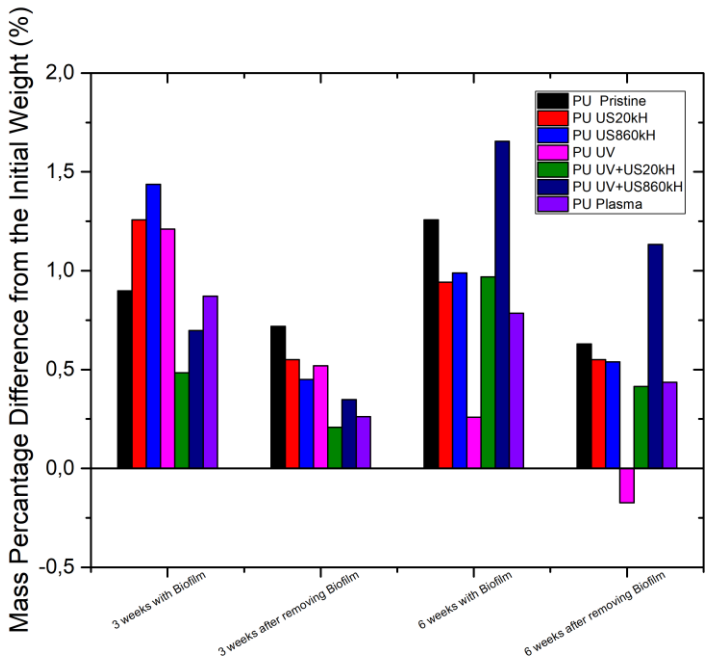

Figure 43: Mass variation of each PU sample after 6 weeks of biodegradation

Figures 42 and 43 illustrate that every pretreatment method favors bacteria adhesion. However, the weight of each sample has increased. Therefore, either the biofilm was not removed entirely or biodegradation was not favored.

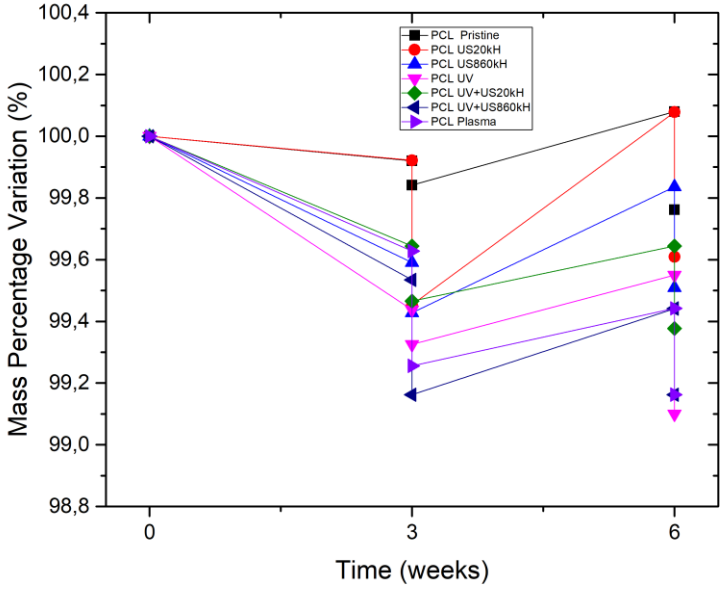

Figure 44: Mass of each PCL sample throughout 6 weeks of biodegradation

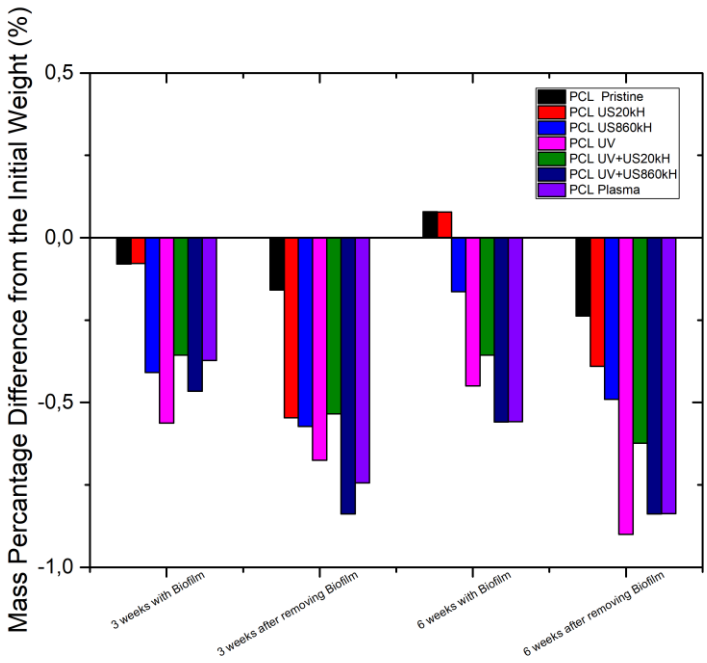

Figure 45: Mass variation of each PCL sample after 6 weeks of biodegradation

Figures 44 and 45 depict that all samples have experienced a weight loss, while after removing the biofilm, the observed weight loss was greater. These results are in accordance with the ones in the first experiment, since in both cases a weight loss is observed. Hence, the average weight loss observed in the first experiment was 3.3 %, whereas in the present experiment it accounted for a 0.6 %. The pretreatment methods which appear to be the most favorable for bacteria adhesion are UV irradiation, combination of UV irradiation and high frequency sonication and plasma treatment.

4th Experiment

As it has been observed in the first two experiments, after the formation of the biofilm, samples have maintained their weight. This result indicates that a new layer of bacteria may facilitate the biodegradation. In this experiment, it is examined whether vigorous agitation could clear the way for new bacteria to attach to the polymer.

PLA samples:

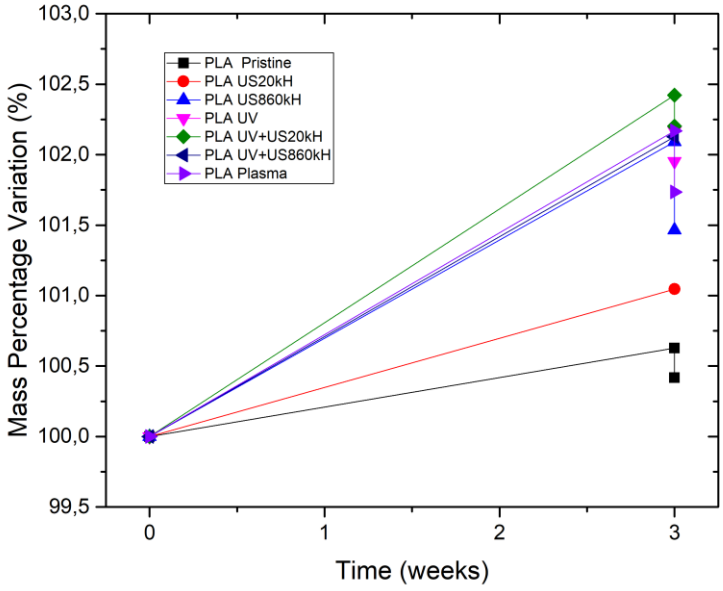

Figure 46: Mass of each PLA sample throughout 3 weeks of biodegradation

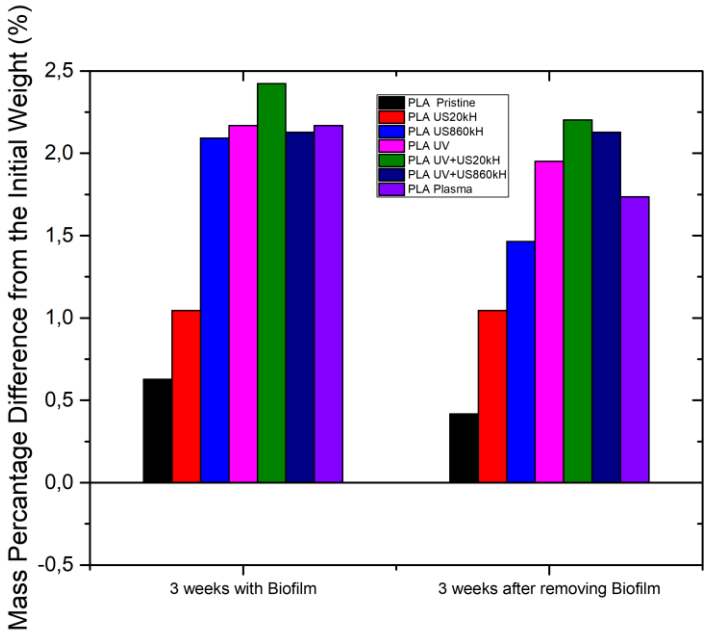

Figure 47: Mass variation of each PLA sample after three weeks of biodegradation.

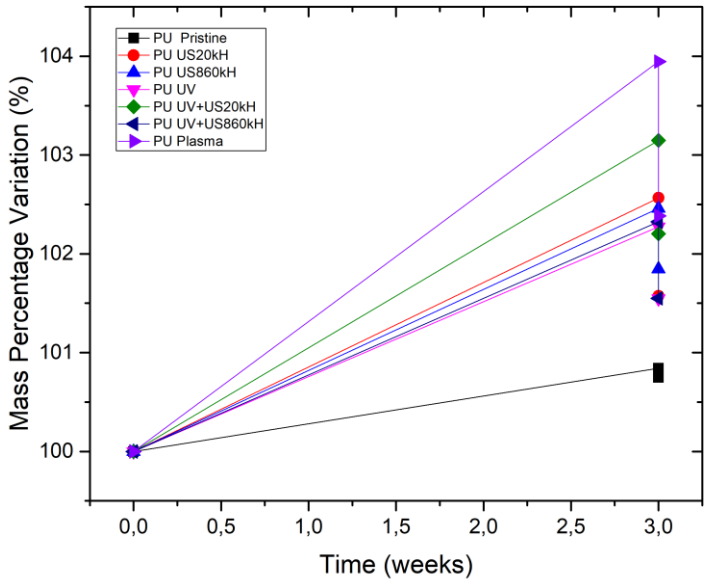

Figure 48: Mass of each PU sample throughout 3 weeks of biodegradation

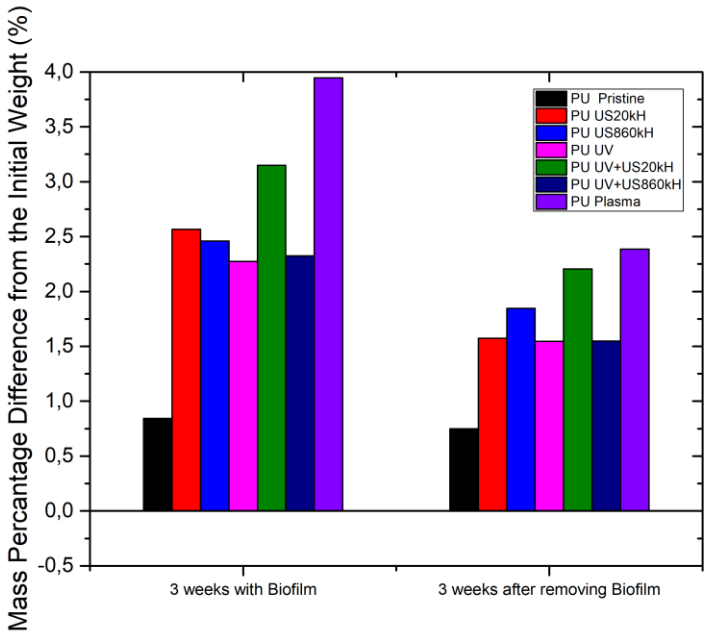

Figure 49: Mass variation of each PU sample after three weeks of biodegradation.

Figures 46, 47, 48, and 49 illustrate that vigorous agitation facilitates the formation of a stronger biofilm, since the average weight increase after three weeks of incubation is greater than the one observed in the previous experiment. More specifically, the average weight increase of PLA samples in the 3rd experiment was 0.8 %, whereas in the present experiment it accounted for a 1.5 %. The PU samples projected a weight increase of almost 1 % with an agitation at 120 rpm, while a 2.5 % weight increase was observed with an agitation at 250 rpm.

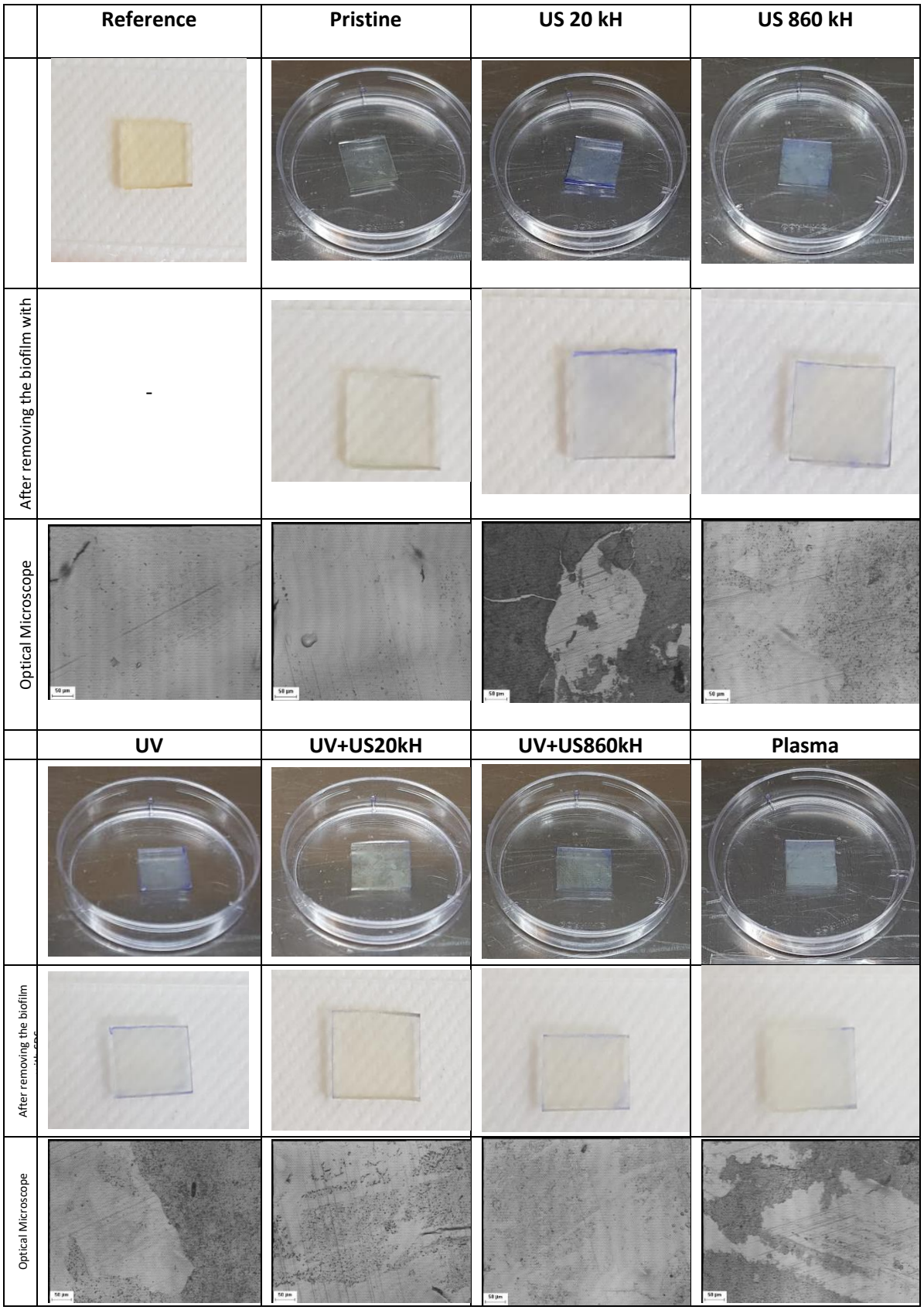

Figure 50: Pictures of the PU samples after exposure to Pseudomonas Knackmussii showing the improved adhesion of the latter as compared to the non-treated (Pristine) sample of PU.

Figure 50 shows that generally the methods which oxidize the surface have a more positive effect on the adhesion of the bacteria on the PU surface, compared to the reference and the untreated (pristine) samples.

From Figures 51 and 52, it is derived that the pretreatment methods which favor adhesion and biodegradation are UV irradiation, combinatorial UV irradiation and high frequency sonication, as well as plasma treatment. Despite the fact that a weight loss is also observed in the first four pretreated samples, it is considered negligible, since it is close to the error limit.

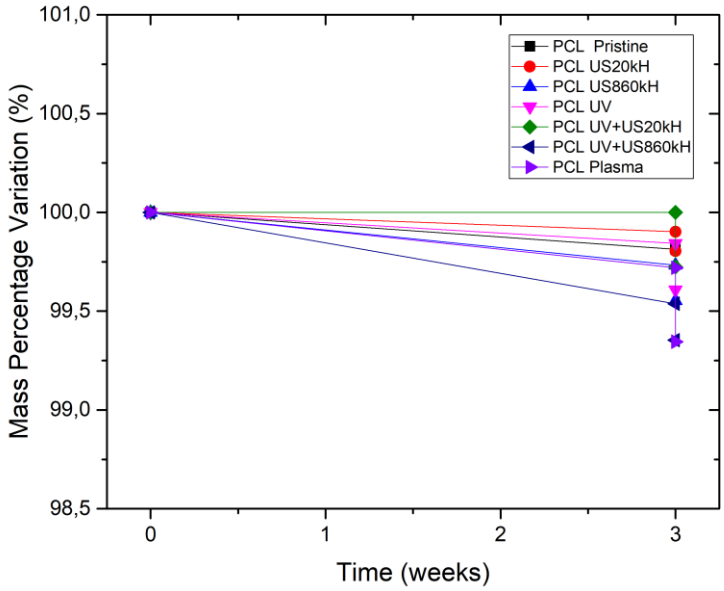

Figure 51: Mass of each PU sample throughout 3 weeks of biodegradation

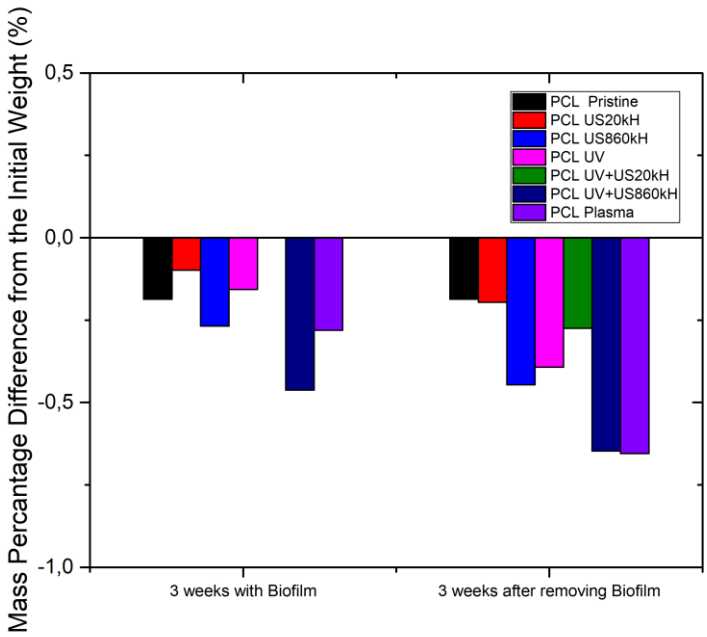

Figure 52: Mass variation of each PCL sample after three weeks of biodegradation.

3.2. FT-IR Results

3.2.1. PLA

FT-IR spectroscopy can be employed so as to confirm the chemical interactions in between the polymer molecules, as well as on the surface of the samples between the polymer and the biofilm. If a chemical interaction exists on the surface, a peak shift or a peak broadening will be shown in the resulting IR spectrum. The IR spectra of the PLA samples are shown in Figures 53, 54, 55 and 56.

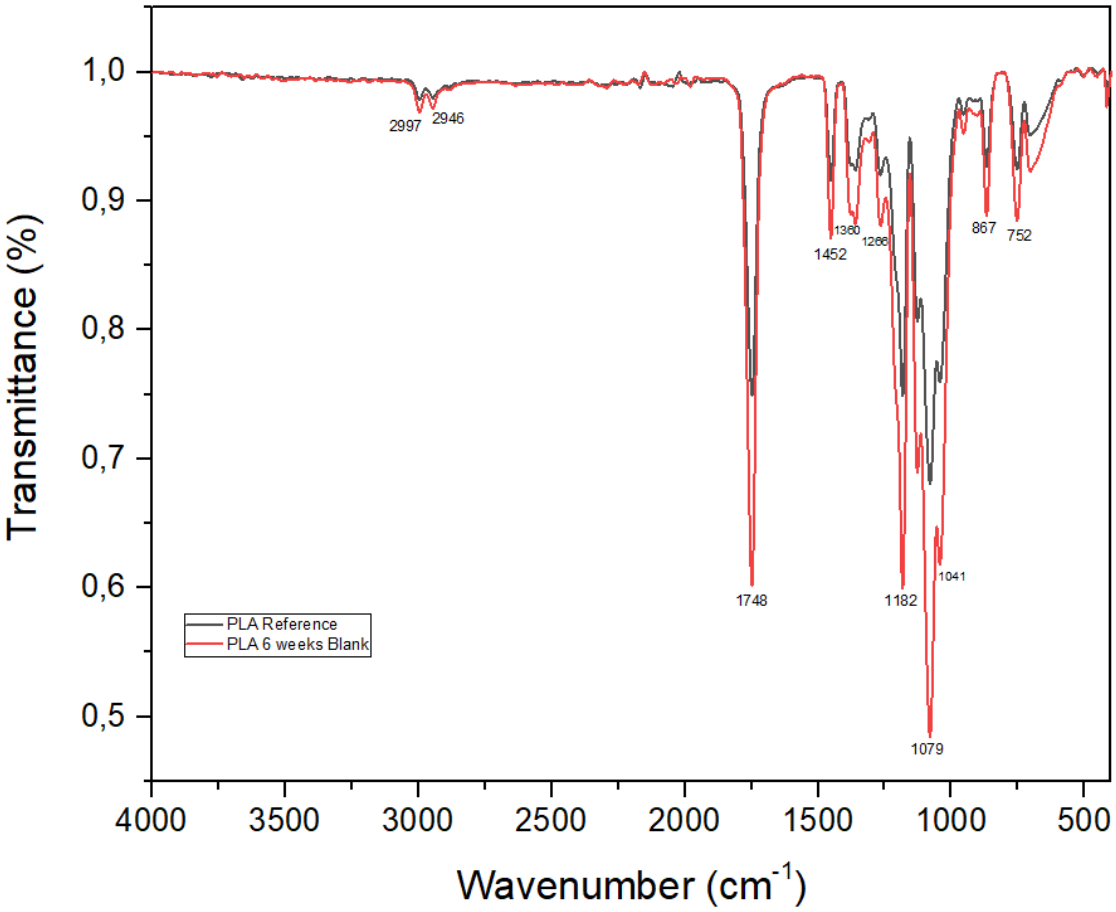

Figure 53: FT-IR Spectrum of the PLA Reference sample and the Blank sample after 6 weeks of biodegradation.

Twelve peaks were identified in the IR spectra of PLA Reference and Blank samples. More specifically, 2997 and 2946 cm^{-1} bands should be assigned as $-\mathrm{C}-\mathrm{H}$ stretching modes. A major band at $1748\,\mathrm{cm}^{-1}$ is the absorption of $\mathrm{C}=\mathrm{O}$ stretching [61]. The 1452 and $1360\,\mathrm{cm}^{-1}$ bands are the asymmetric and symmetric bending absorptions of $-\mathrm{CH}_3$, respectively. The bands from 1266 to $1041\,\mathrm{cm}^{-1}$ correspond to the stretching absorptions of the ester bond ($\mathrm{C}-\mathrm{O}-\mathrm{C}$). Their proximity can be justified due to different atoms of function groups adjoining to $\mathrm{C}-\mathrm{O}-\mathrm{C}$. Pointedly, the $1182\,\mathrm{cm}^{-1}$ band is an ester $-\mathrm{C}-\mathrm{O}-$ symmetric stretch and the one at $1079\,\mathrm{cm}^{-1}$ is an asymmetric $-\mathrm{C}-\mathrm{O}-\mathrm{C}-$ stretch [61]. The $867\,\mathrm{cm}^{-1}$ band should be ascribed to the amorphous phase of PLA, whilst the $752\,\mathrm{cm}^{-1}$ is attributed to its crystalline phase.

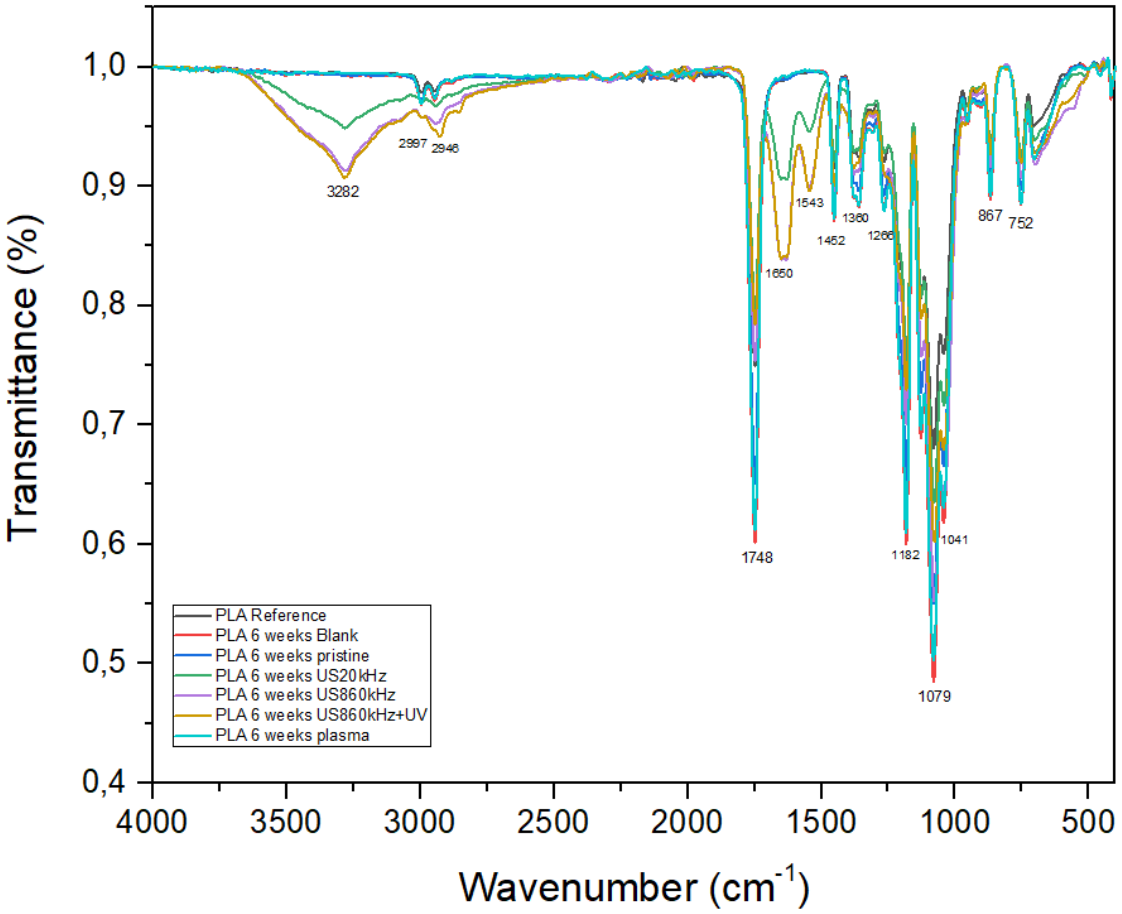

Figure 54: FT-IR of PLA samples after 6 weeks of biodegradation.

Fifteen peaks were identified in the IR spectra of PLA samples. More specifically, there are three additional peaks that can be observed in PLA samples that have undergone incubation for 6 weeks, at 3282, 1650 and $1543\ \mathrm{cm}^{-1}$. The $3282\ \mathrm{cm}^{-1}$ band should be assigned as an $-\mathrm{OH}$ peak on stretching mode. That $-\mathrm{OH}$ broad stretching corresponds to either an acid, probably originated from the acetic acid or a free hydroxyl group. The $1650\ \mathrm{cm}^{-1}$ medium band can be attributed to $\mathrm{N}-\mathrm{H}$ bending, most likely because of the amine groups that are present on the active site of the enzymes which interact with the sample surface to hydrolyze the polymer. At $1650\ \mathrm{cm}^{-1}$ there are two peaks in close proximity which almost overlap. This could also be assigned to an $\mathrm{O}-\mathrm{H}$ bending from absorbed water molecules [61]. The $1543\ \mathrm{cm}^{-1}$ band can describe a $\mathrm{N}-\mathrm{O}$ stretching. In general, the range between 1500 and $1600\ \mathrm{cm}^{-1}$ is typically where the peaks of nitrogen compounds are found. Another explanation to the presence of nitrogen groups could be the existence of nitrogen atoms in the crystal violet solution used to stain the biofilm. The samples which illustrate the greatest transmittance are US20kH, US860kH US860kH+UV samples.

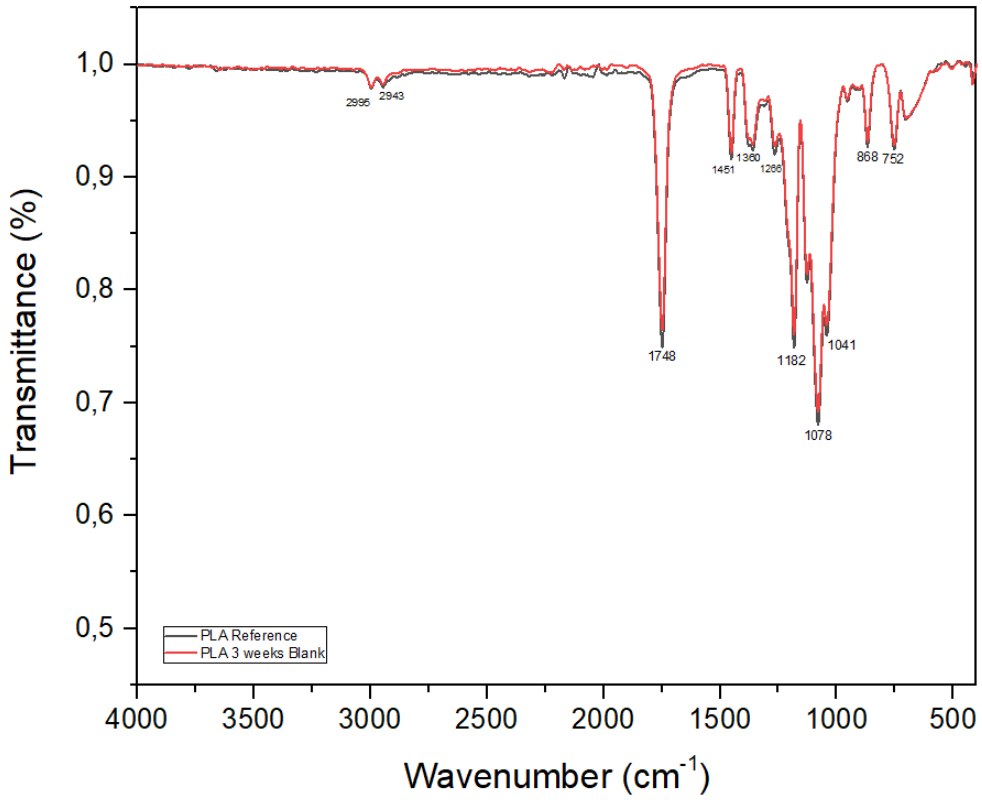

Figure 55: FT-IR Spectrum of the PLA Reference sample and the Blank sample after 3 weeks of biodegradation.

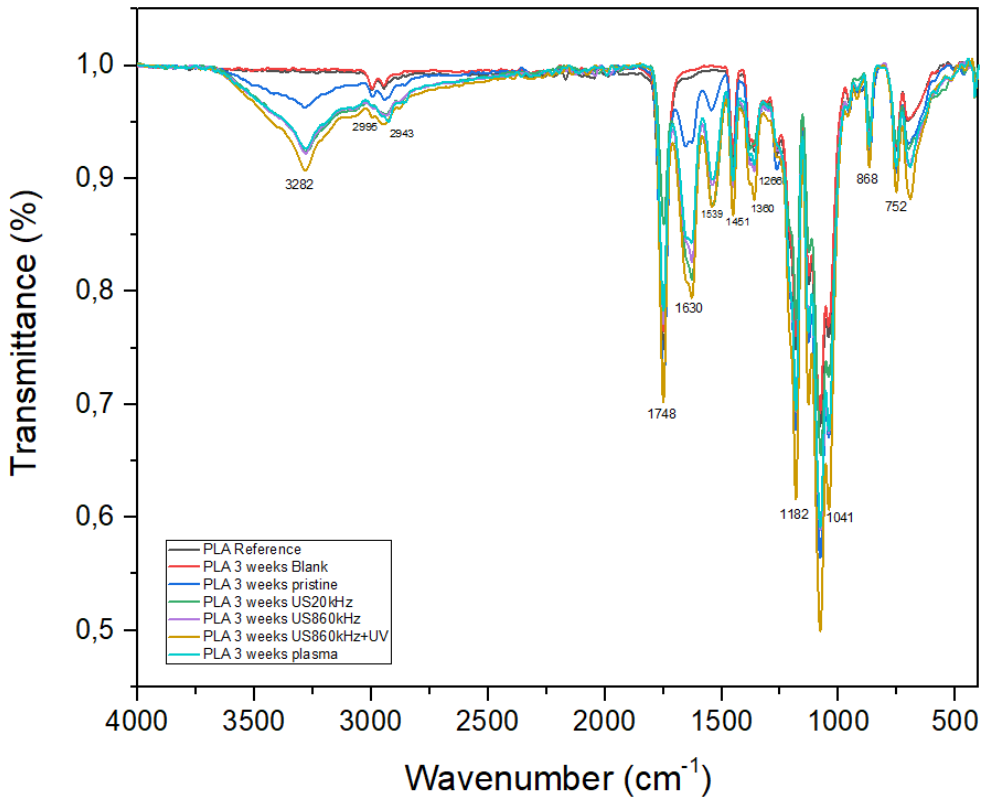

Figure 56: FT-IR Spectrum of PLA samples after 3 weeks of biodegradation.

The derived spectra from the samples which have undergone 3 weeks of biodegradation almost coincided with the previous ones. A notable difference in this Figure is that, except the Reference and the Blank samples, the ones that have been treated with bacteria illustrate a significantly greater transmittance in these three differentiating bands. The samples which illustrate the greatest transmittance are US20kH, US860kH, US860kH+UV and plasma samples.

3.2.2. PCL

The IR spectra of the PCL samples are shown in Figures 57, 58, 59 and 60.

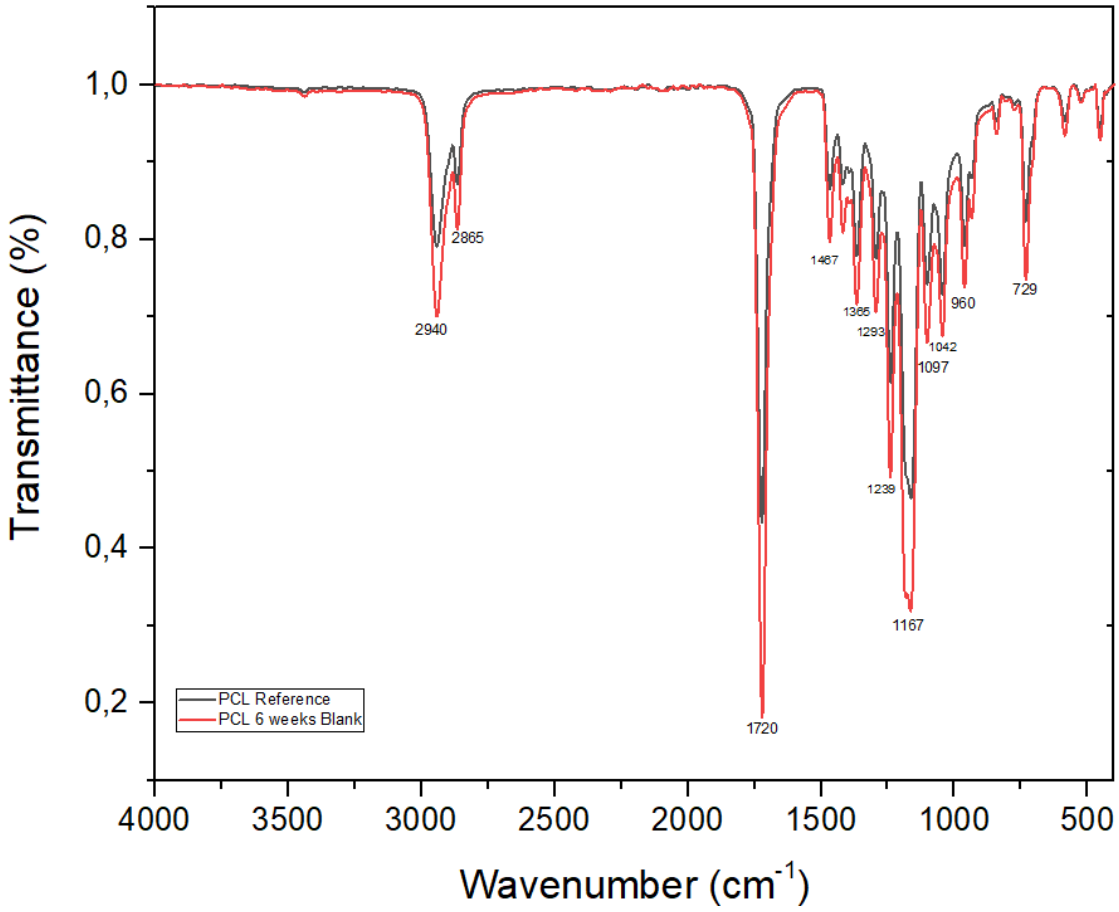

Figure 57: FT-IR Spectrum of the PCL Reference sample and the Blank sample after 6 weeks of biodegradation.

The PCL spectrum illustrates similar bands in similar positions compared to the PLA spectra. More specifically, the two peaks which appear at 2940 and $2865\ \mathrm{cm}^{-1}$ correspond to asymmetric CH_2 stretching and symmetric CH_2 stretching, respectively [62]. The most characteristic bands of the PCL are the carbonyl stretching at $1720\ \mathrm{cm}^{-1}$, the bending modes of CH_2 at 1365, 1417 and $1467\mathrm{cm}^{-1}$, the asymmetric COC stretching at 1097, $1239\ \mathrm{cm}^{-1}$, the $C-O$ and $C-C$ stretching in crystalline phase $1293\ \mathrm{cm}^{-1}$ and the $C-O$ and $C-C$ stretching in the amorphous phase at $1167\ \mathrm{cm}^{-1}$ [62]. The band at $572\ \mathrm{cm}^{-1}$ can be assigned to the in-plane and out-of-plane deformations of the carbonyl group [63].

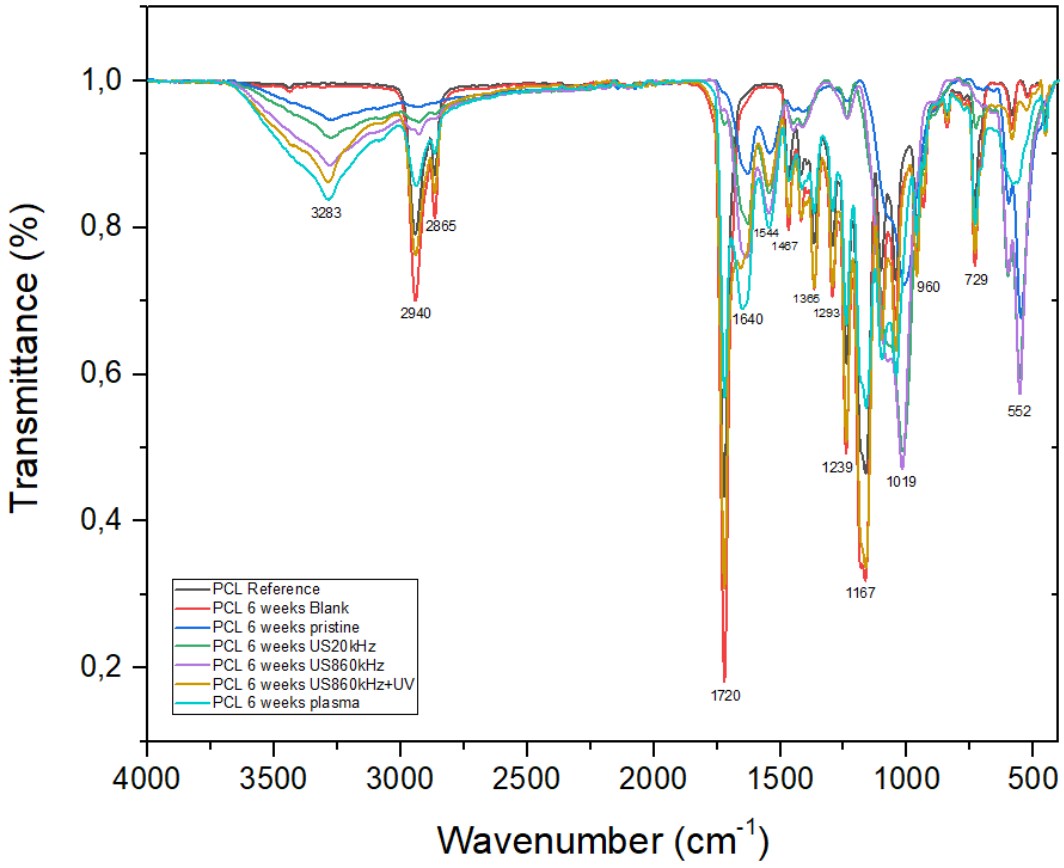

Figure 58: FT-IR of PCL samples after 6 weeks of biodegradation.

The incubated PCL samples demonstrate three additional peaks at 3283, 1640 and $1544\ \mathrm{cm}^{-1}$, similarly to the incubated PLA samples. The peak at $3283\ \mathrm{cm}^{-1}$ is assigned to the stretching vibration of the OH group. The $1640\ \mathrm{cm}^{-1}$ band is attributed to $\mathrm{N-H}$ bending and the one at $1544\ \mathrm{cm}^{-1}$ to a $\mathrm{N-O}$ stretching. The samples which illustrate the most intense peaks are the plasma-pretreated sample, the high frequency sonicated sample as well as the combinatorially UV irradiated and high frequency ultrasonicated sample.

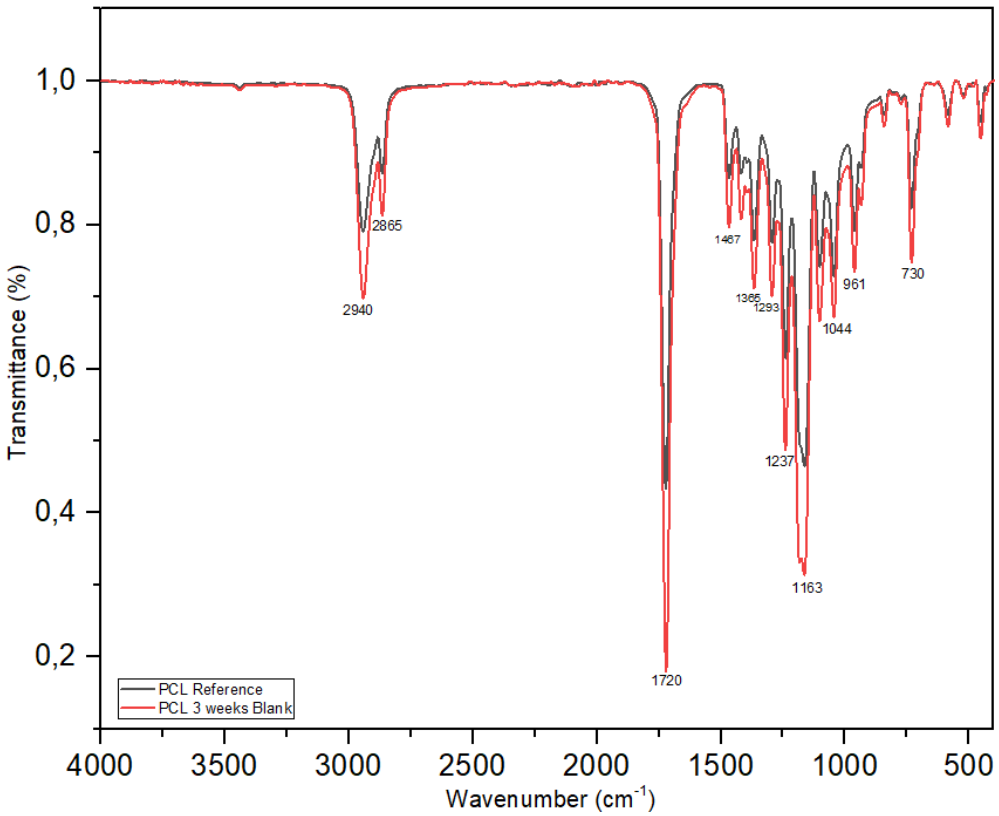

Figure 59: FT-IR Spectrum of the PCL Reference sample and the Blank sample after 3 weeks of biodegradation.

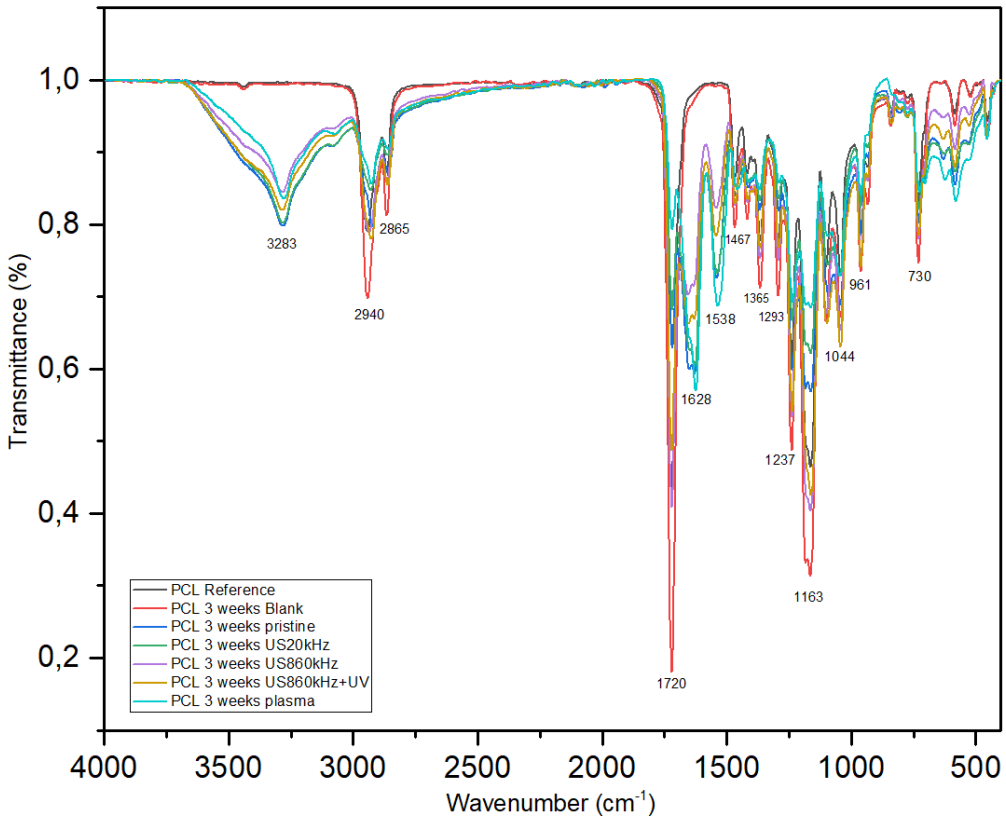

Figure 60: FT-IR of PCL samples after 3 weeks of biodegradation.

The spectra of the PCL samples which have undergone 3 weeks of biodegradation are identical with the ones that have undergone 6 weeks of biodegradation. Except the reference and Blank samples, the rest of them illustrate the additional peaks very intensely.

In general, the additional peaks which appear in the PLA and PCL spectra of the incubated samples almost coincide. This can be assigned to the strain and the conditions that where necessary for the cultivation of the strain.

3.3. CLSM

The evaluation of the mass variation and the IR spectra indicated that PLA and PCL samples have undergone preliminary degradation. Examination of their surface can bear stronger evidence of how bacteria have acted. Therefore, CLSM measurements were held. The values that are more meaningful in order to characterize their surface roughness are Ra and Rq.

Table 19: CLSM results for s for the surface roughness.

SAMPLE	CONDITIONS	TREATMENT		
			Ra (nm)	Rq (nm)
PLA	6 weeks at 120 rpm	Blank	7.945	32.058
		Pristine	16.114	52.777
		US20kHz	4.197	18.219
		US860KHz	4.010	5.377
		US860KHz+UV	3.972	16.236
		plasma	18.847	51.354
	3 weeks at 250 rpm	Blank	3.568	4.312
		Pristine	2.474	4.081
		US20kHz	3.042	4.073
		US860KHz	4.453	6.592
		US860KHz+UV	4.566	5.672
		plasma	3.540	4.501
PCL	6 weeks at 120 rpm	Blank	4.446	5.419
		Pristine	4.739	5.934
		US20kHz	4.495	5.726
		US860KHz	3.728	4.679
		US860KHz+UV	4.593	5.717
		plasma	14.228	16.984
	3 weeks at 250 rpm	Blank	3.184	3.938
		Pristine	10.049	11.877
		US20kHz	13.165	15.567
		US860KHz	8.750	10.217
		US860KHz+UV	4.927	5.389
		plasma	5.488	6.755

In the collected samples from Experiments 3 and 4 show that, in general, the roughness of every sample has increased, due to the formation of bacterial colonies. The results from the 3rd Experiment in PLA degradation are unreliable, since the Rq value of the blank sample is high. That corresponds to high standard deviation. The results from PCL showed that every sample has an increased roughness, except the high frequency sonicated sample. Especially the plasma treated sample has a high Ra value, a result that is in accordance with its extensive weight loss. The UV+US860kH sample showed a slightly increased roughness. This result implies that the biofilm was not removed entirely. It is important to note that, because of the

way the measurements are performed, sometimes the part that is being analyzed is not relevant to the entire surface of the sample.

In the 4th Experiment, pristine and US20kH PLA samples have become smoother. US860kH and US860kH+UV have become rougher, while the plasma treated sample's surface remained stable. Regarding the PCL samples, every sample possessed a rougher surface after the bacteria adhesion. Plasma and UV+US860kH samples, which illustrated the greatest weight loss, had a relatively lower roughness compared to the other samples.

CLSM provided the following images. Figure 61 and 63 show the blank PLA and PCL samples, which have undergone incubation without bacteria. It is evident that their surface is clear. On the contrary, Figures 62 and 64 show the sonicated at 20kH and a plasma pretreated sample. It is obvious that the pre-treatment has a positive influence on the adhesion of the strain *Pseudomonas knackmussii*. The surface percentage covered depends on the treatment method. Methods that oxidize the surface have a positive effect on the adhesion of the bacteria on the PLA surface.

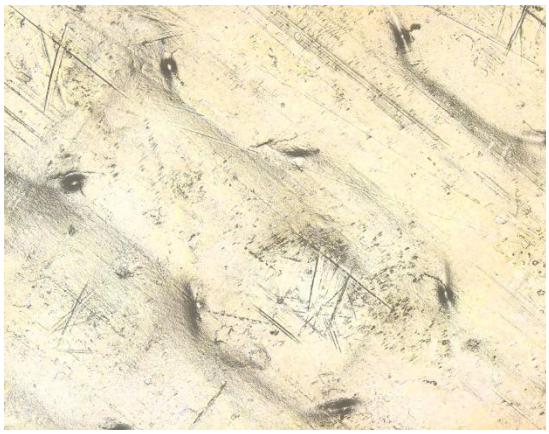

Figure 61: PLA blank sample – CLSM image

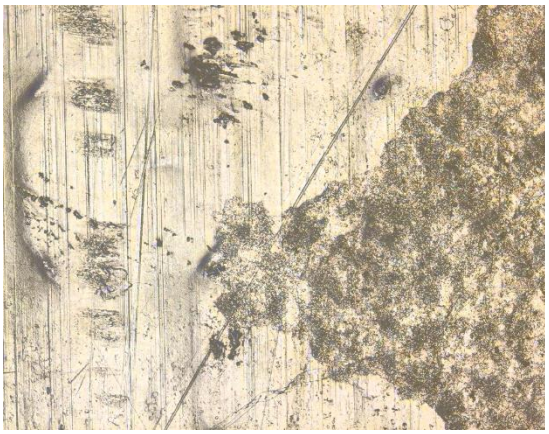

Figure 62: US 20 kH PLA sample – CLSM image

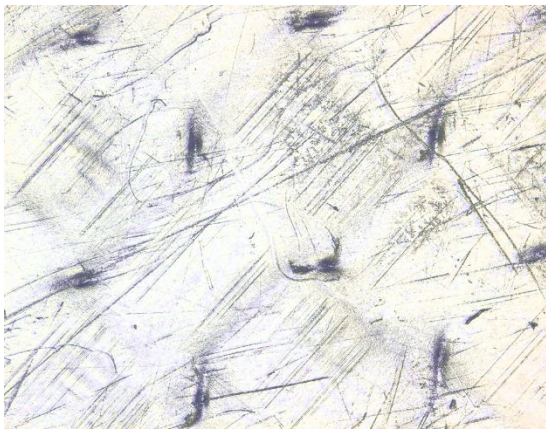

Figure 63: PCL blank sample – CLSM image

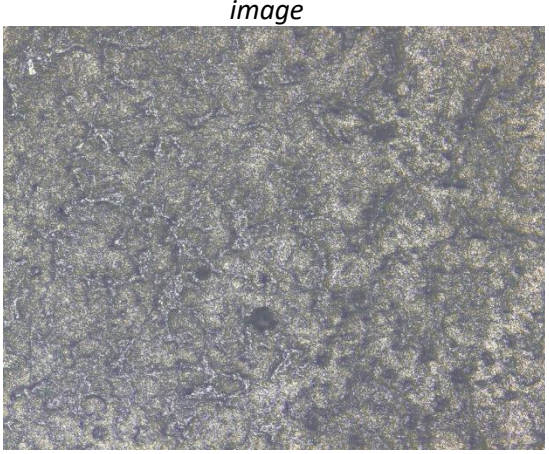

Figure 64: PCL Plasma sample – CLSM image.

4. DISCUSSION AND CONCLUSIONS

The 1st and the 2nd Experiment were performed mainly as preliminary experiments that would give insight into whether bacteria adhesion occurs using two different strains. Results derived from the 2nd Experiment showed that the strain *P. Umsongensis* can be attached on the surface of the polymers, but it does not degrade. The growth ratios indicate that either contamination had occurred or the starvation should have been more stringent. Results from the 1st Experiment depicted that bacterial adhesion of *P. Knackmussii* on the surface of all three polymers occurs, while degradation of PCL was observed. However, after the first week of degradation the weight of the PCL samples increased. It was hypothesized that the biofilm docked on the surface should be renewed in order for the biodegradation to continue.

The 3rd Experiment was conducted to shed light on whether biodegradation could go further by extending the time of incubation. The 4th Experiment was conducted to scrutinize whether vigorous agitation could clear the way for fresh bacteria to attach on the polymer substrate.

Regarding the PLA samples, results from the 3rd Experiment showed that only plasma treated and sonicated at $20\mathrm{kH}$ samples exhibited a quantifiable weight loss, amounting 0.64 and $0.60\ \%$, respectively. At first glance, this weight loss could be considered insignificant. However, similar experiments performed using a single microorganism, illustrated a comparable weight loss. More specifically, after inoculating PLA samples with the fungus *Trichoderma viride* at $28\ ^{\circ}\mathrm{C}$ for 3 weeks, a weight loss of $1.2\ \%$ was observed [64]. Composting can achieve remarkably higher weight loss (77%), mainly due to the fact that the biodegradation is conducted by consortia of microbes at higher temperatures ($\mathrm{T} > 58\ ^{\circ}\mathrm{C}$) [65], while low temperature composting results in less than $3\ \%$ biodegradation [66].

The IR spectrum of the sonicated at $20\mathrm{kH}$ sample exhibited three additional peaks compared to the reference sample, which correspond to OH radicals and nitrogen compounds. The IR spectrum of the plasma treated sample did not exhibit these additional peaks, probably because the biofilm was successfully removed. Results from the 4th Experiment rejected the idea that vigorous shaking would facilitate the surface's renewal with bacteria. On the contrary, a more resilient biofilm was formed, which was challenging to remove with the SDS detergent. After partially removing it, every sample exhibited an increased weight compared to their initial ones. Moreover, the IR spectra of every sample exhibited the same three additional peaks which are attributed to OH radicals and nitrogen compounds. Therefore, it is observed that when the biofilm is not removed properly, these peaks appear, so they could be related to nitrogen atoms present in enzymes responsible for hydrolyzing the polymer.

Regarding the PU samples, a weight increase is serially observed in both the 3rd and 4th experiment. All pretreatment methods favor the bacteria adhesion. Hence, since the complete removal of the biofilm is challenging, no clear statement can be made as to whether biodegradation occurs. Evidently, the culture media were contaminated, because the sterilization of the samples was deficient. What is more, considering the vast number of samples that were to be examined, FT-IR analysis was not conducted in PU samples.

Regarding the PCL samples, the 3.3 % average weight loss observed in the 1st experiment was equivocal, since repetition showed that this observation was never repeated in the following experiments. Results from the 3rd Experiment showed that plasma treated, UV irradiated and combinatorially UV irrariated high frequency sonicated samples exhibited a quantifiable weight loss, pertaining to 0.89, 0.83 and 0.83 %, respectively. Results from the 4th Experiment showed that plasma treated and UV+US860kH samples exhibited a significant weight loss, pertaining to 0.65 and 0.64 %, respectively. Similar experiments conducted with a single strain illustrated a comparable weight loss at a higher temperature. Specifically, neat PCL samples incubated at 37 ℃ for 2 weeks with the strain *Pseudomonas aeruginosa* PAO1 showed a 4.3 % weight decrease [67]. Similar to the PLA biodegradation, composting of PCL illustrates more significant weight loss due to the presence of a variety of bacteria at higher temperatures. For instance, PCL powder that was introduced in a compost mixture at 50℃ was completely assimilated after 100 days [68]. However, the same experiment conducted at 25 ℃ showed a 25 % weight decrease after 100 days. In general, it is reported that symbiotic relationship between strains can facilitate the plastic degradation. Specifically, the biofilm formed by bacteria *Bacillus mycoides* and *Penicillium frequentans* on the surface of degradable polyethylene samples reduced the weight of the plastic by 7% [69]. Thus, when isolating each strain, the degradation results were less promising, since the weight loss observed with the individual strain of *P. frequentans* and *B. mycoides* was 0.45 to 0.50% and 0.01%, respectively.

Comparing the IR spectra of these samples (which are similar to PLA), it is evident that plasma treated samples illustrate the sharpest peaks which correspond to OH radicals and nitrogen compounds.

CLSM results show that generally after the incubation the roughness has increased, most likely because of the presence of bacteria. There are some results that do not confirm this statement. This could be justified, since, during a measurement, the roughness is calculated only for a small part (in nm) of the whole surface of the sample.

It has been reported that PLA and PCL show a low rate of degradation in neutral environment, whilst the degradation activity is improved in basic and acidic conditions [31]. The aforementioned experiments were held in relatively neutral environment, since the culture media had a pH value of 7.

5. FUTURE RESEARCH STEPS

The results of this diploma thesis show that in order for the biodegradation to be more efficient, some additional experiments should be held to determine the optimum starvation concentration. More specifically, the 3rd Experiment can be repeated with a more drastic starvation, by adding peptone at a lower concentration (e.g. $5\ \%$ PM medium). That way bacteria will be probably forced to digest the polymer.

Another similar approach would be to cultivate the strain *P. Knackmussii* at a concentration less than $5\ \%$ PM medium for a month with the simultaneous presence of plastic samples. Most of the cells will die. The ones that will survive will be collected via centrifugation. These cells are likely to have develop the ability to digest plastic. The viability of the cells can be verified with the absorbance as well as COD (Chemical Oxygen Demand: measure of the amount of oxygen that can be consumed) measurements. It is strongly recommended for the above experiment to be conducted in triplicate.

PU samples exhibited a peculiarity related to sterilization, since dipping them in $80\ \%$ ethanol was inadequate. Therefore, UVC irradiation for $5\ \mathrm{min}$ is recommended due to its efficacy as a germicidal agent.

In many cases the biofilm was partially removed with 2% SDS. Therefore, either a higher concentration of SDS can be applied or another detergent should be used, such as tween20. An alternative way to remove the biofilm would be sonication for $5\ \mathrm{min}$. The samples will be placed in flasks filled with demineralized water and sonicated in an ultrasonics bath.

The strain *Pseudomonas umsongensis* illustrated the least promising results. However, repetition of the 2nd Experiment with a lower concentration of peptone is recommended.

Further analysis of the culture medium will shed light on whether the polymer is degraded. More specifically, the culture medium can be separated from the cells through centrifugation and then injected to chromatography. HPLC coupled with a UV detector is a method suitable for the qualitative analysis of oligomers derived from the depolymerized plastic.

Moreover, XPS analysis of the surface of the samples is recommended as a rational approach to derive quantitative and chemical state information for studied surface. Additionally, Drop Contour Analysis (DCA) can be performed to characterize the wettability of the surfaces.

Furthermore, SEM measurements will provide useful pictures of the way the bacteria are attached on the sample's surface.

6. REFERENCES

[1] British Plastics Federation, “Oil consumption,” *British Plastics Federation*. [Online]. Available: https://www.bpf.co.uk/press/Oil_Consumption.aspx. [Accessed: 11-Sep-2022].

[2] R. Geyer, “A brief history of plastics,” Mare Plasticum - The Plastic Sea, pp. 31–47, 2020.

[3] T. Narancic and K. E. O'Connor, “Plastic waste as a global challenge: Are biodegradable plastics the answer to the plastic waste problem?,” Microbiology, vol. 165, no. 2, pp. 129–137, 2019.

[4] Y. Zheng, E. K. Yanful, and A. S. Bassi, “A review of Plastic Waste Biodegradation,” Critical Reviews in Biotechnology, vol. 25, no. 4, pp. 243–250, 2005.

[5] Y. Loganathan and M. P. J. Kizhakedathil , “A review on microplastics – an indelible ubiquitous pollutant,” Biointerface Research in Applied Chemistry, vol. 13, no. 2, p. 126, 2022.

[6] V. Shanmugam, O. Das, R. E. Neisiany, K. Babu, S. Singh, M. S. Hedenqvist, F. Berto, and S. Ramakrishna, “Polymer recycling in Additive Manufacturing: An opportunity for the circular economy,” Materials Circular Economy, vol. 2, no. 1, 2020.

[7] S. Sid, R. S. Mor, A. Kishore, and V. S. Sharanagat, “Bio-sourced polymers as alternatives to conventional food packaging materials: A Review,” Trends in Food Science & Technology, vol. 115, pp. 87–104, 2021

[8] “Bioplastics,” European Bioplastics e.V., 23-May-2022. [Online]. Available: https://www.european-bioplastics.org/bioplastics/. [Accessed: 12-Sep-2022]

[9] E. Nikolaivits, B. Pantelic, M. Azeem, G. Taxeidis, R. Babu, E. Topakas, M. Brennan Fournet, and J. Nikodinovic-Runic, “Progressing plastics circularity: A review of mechano-biocatalytic approaches for waste plastic (re)valorization,” Frontiers in Bioengineering and Biotechnology, vol. 9, 2021.

[10] T. Narancic, S. Verstichel, S. Reddy Chaganti, L. Morales-Gamez, S. T. Kenny, B. De Wilde, R. Babu Padamati, and K. E. O’Connor, “Biodegradable plastic blends create new possibilities for end-of-life management of plastics but they are not a panacea for plastic pollution,” Environmental Science & Technology, vol. 52, no. 18, pp. 10441–10452, 2018

[11] O. Avinc and A. Khoddami, “Overview of poly(lactic acid) (PLA) fibre,” Fibre Chemistry, vol. 41, no. 6, pp. 391–401, 2009.

[12] R. M. Mohamed and K. Yusoh, “A review on the recent research of Polycaprolactone (PCL),” Advanced Materials Research, vol. 1134, pp. 249–255, 2015.

[13] V. Guarino, G. Gentile, L. Sorrentino, and L. Ambrosio, “Polycaprolactone: Synthesis, properties, and applications,” Encyclopedia of Polymer Science and Technology, pp. 1–36, 2017

[14] J. O. Akindoyo, M. D. Beg, S. Ghazali, M. R. Islam, N. Jeyaratnam, and A. R. Yuvaraj, “Polyurethane types, synthesis and applications – A Review,” RSC Advances, vol. 6, no. 115, pp. 114453–114482, 2016.

[15] G. T. Howard, “Biodegradation of polyurethane: A Review,” International Biodeterioration & Biodegradation, vol. 49, no. 4, pp. 245–252, 2002.

[16] M. Liu, S. Lu, Y. Song, L. Lei, J. Hu, W. Lv, W. Zhou, C. Cao, H. Shi, X. Yang, and D. He, “Microplastic and mesoplastic pollution in farmland soils in suburbs of Shanghai, China,” Environmental Pollution, vol. 242, pp. 855–862, 2018

[17] J. Yang, L. Li, R. Li, L. Xu, Y. Shen, S. Li, C. Tu, L. Wu, P. Christie, and Y. Luo, “Microplastics in an agricultural soil following repeated application of three types of sewage sludge: A field study,” Environmental Pollution, vol. 289, p. 117943, 2021

[18] P. C. Deshpande, G. Philis, H. Brattebø, and A. M. Fet, “Using material flow analysis (MFA) to generate the evidence on plastic waste management from commercial fishing gears in Norway,” Resources, Conservation & Recycling: X, vol. 5, p. 100024, 2020.

[19] M. Eriksen, L. C. Lebreton, H. S. Carson, M. Thiel, C. J. Moore, J. C. Borerro, F. Galgani, P. G. Ryan, and J. Reisser, “Plastic pollution in the world's oceans: More than 5 trillion plastic pieces weighing over 250,000 tons afloat at sea,” PLoS ONE, vol. 9, no. 12, 2014.

[20] A. Rahman, A. Sarkar, O. P. Yadav, G. Achari, and J. Slobodnik, “Potential human health risks due to environmental exposure to nano- and microplastics and knowledge gaps: A scoping review,” Science of The Total Environment, vol. 757, p. 143872, 2021.

[21] A. Tamargo, N. Molinero, J. J. Reinosa, V. Alcolea-Rodriguez, R. Portela, M. A. Bañares, J. F. Fernández, and M. V. Moreno-Arribas, “Pet microplastics affect human gut microbiota communities during simulated gastrointestinal digestion, first evidence of plausible polymer biodegradation during human digestion,” Scientific Reports, vol. 12, no. 1, 2022.

[22] “Circular economy: Definition, importance and benefits: News: European parliament,” Circular economy: definition, importance and benefits | News | European Parliament, 26-Apr-2022. [Online]. Available: https://www.europarl.europa.eu/news/en/headlines/economy/20151201STO05603/circular-economy-definition-importance-and-benefits. [Accessed: 12-Sep-2022].

[23] A. Hodzic, “Re-use, recycling and degradation of Composites,” Green Composites, pp. 252–271, 2004.

[24] G. Kale, T. Kijchavengkul, R. Auras, M. Rubino, S. E. Selke, and S. P. Singh, “Compostability of bioplastic packaging materials: An overview,” Macromolecular Bioscience, vol. 7, no. 3, pp. 255–277, 2007.

[25] N. Mohanan, Z. Montazer, P. K. Sharma, and D. B. Levin, “Microbial and enzymatic degradation of synthetic plastics,” Frontiers in Microbiology, vol. 11, 2020.

[26] J. A. Glaser, “Biological degradation of polymers in the environment,” Plastics in the Environment, 2019.

[27] R.-S. Rose, K. H. Richardson, E. J. Latvanen, C. A. Hanson, M. Resmini, and I. A. Sanders, “Microbial degradation of plastic in aqueous solutions demonstrated by CO2 evolution and quantification,” International Journal of Molecular Sciences, vol. 21, no. 4, p. 1176, 2020.

[28] C. Charnock, “A simple and novel method for the production of polyethylene terephthalate containing agar plates for the growth and detection of bacteria able to hydrolyze this plastic,” Journal of Microbiological Methods, vol. 185, p. 106222, 2021.

[29] E. Nikolaivits, P. Dimopoulou, V. Maslak, J. Nikodinovic-Runic, and E. Topakas, “Discovery and biochemical characterization of a novel polyesterase for the degradation of synthetic plastics,” The 1st International Electronic Conference on Catalysis Sciences, 2020.

[30] V. Pathak and Navneet, “Review on the current status of polymer degradation: A microbial approach,” Bioresources and Bioprocessing, vol. 4, no. 1, 2017.

[31] Shilpa, N. Basak, and S. S. Meena, “Microbial biodegradation of plastics: Challenges, opportunities, and a critical perspective,” Frontiers of Environmental Science & Engineering, vol. 16, no. 12, 2022.

[32] A. Magnin, E. Pollet, V. Phalip, and L. Avérous, “Evaluation of biological degradation of polyurethanes,” *Biotechnology Advances*, vol. 39, p. 107457, 2020.

[33] S. Yoshida, K. Hiraga, T. Takehana, I. Taniguchi, H. Yamaji, Y. Maeda, K. Toyohara, K. Miyamoto, Y. Kimura, and K. Oda, “A bacterium that degrades and assimilates poly(ethylene terephthalate),” Science, vol. 351, no. 6278, pp. 1196–1199, 2016.

[34] P. Liu, T. Zhang, Y. Zheng, Q. Li, T. Su, and Q. Qi, “Potential One-step strategy for PET degradation and PHB biosynthesis through co-cultivation of two engineered microorganisms,” *Engineering Microbiology*, vol. 1, p. 100003, 2021.

[35] J. Liu, J. He, R. Xue, B. Xu, X. Qian, F. Xin, L. M. Blank, J. Zhou, R. Wei, W. Dong, and M. Jiang, “Biodegradation and up-cycling of polyurethanes: Progress, challenges, and prospects,” Biotechnology Advances, vol. 48, p. 107730, 2021.

[36] H. Lu, D. J. Diaz, N. J. Czarnecki, C. Zhu, W. Kim, R. Shroff, D. J. Acosta, B. R. Alexander, H. O. Cole, Y. Zhang, N. A. Lynd, A. D. Ellington, and H. S. Alper, “Machine learning-aided engineering of hydrolases for pet depolymerization,” Nature, vol. 604, no. 7907, pp. 662–667, 2022.

[37] S. Teixeira, K. M. Eblagon, F. Miranda, M. F. R. Pereira, and J. L. Figueiredo, “Towards controlled degradation of poly(lactic) acid in technical applications,” C, vol. 7, no. 2, p. 42, 2021.

[38] M. Ponjavic, M. S. Nikolic, J. Nikodinovic-Runic, S. Jeremic, S. Stevanovic, and J. Djonlagic, “Degradation behaviour of PCL/PEO/PCL and PCL/PEO Block Copolymers under

controlled hydrolytic, enzymatic and composting conditions," Polymer Testing, vol. 57, pp. 67–77, 2017.

[39] S. Bahl, J. Dolma, J. Jyot Singh, and S. Sehgal, "Biodegradation of plastics: A state of the art review," Materials Today: Proceedings, vol. 39, pp. 31–34, 2021.

[40] M. Bartnikowski, T. R. Dargaville, S. Ivanovski, and D. W. Hutmacher, "Degradation mechanisms of polycaprolactone in the context of chemistry, geometry and environment," Progress in Polymer Science, vol. 96, pp. 1–20, 2019.

[41] L. Hedstrom, "Serine protease mechanism and specificity," Chemical Reviews, vol. 102, no. 12, pp. 4501–4524, 2002.

[42] G. Sourkouni, C. Kalogirou, P. Moritz, A. Gödde, P. K. Pandis, O. Höfft, S. Vouyiouka, A. A. Zorpas, and C. Argirusis, "Study on the influence of advanced treatment processes on the surface properties of polylactic acid for a bio-based circular economy for plastics," Ultrasonics Sonochemistry, vol. 76, p. 105627, 2021.

[43] G. McHale, N. J. Shirtcliffe, and M. I. Newton, "Contact-angle hysteresis on super-hydrophobic surfaces," Langmuir, vol. 20, no. 23, pp. 10146–10149, 2004.

[44] J. P. Mofokeng, A. S. Luyt, T. Tábi, and J. Kovács, "Comparison of injection moulded, natural fibre-reinforced composites with PP and PLA as matrices," Journal of Thermoplastic Composite Materials, vol. 25, no. 8, pp. 927–948, 2011.

[45] B. T. Ho, T. K. Roberts, and S. Lucas, "An overview on biodegradation of polystyrene and modified polystyrene: The Microbial Approach," Critical Reviews in Biotechnology, vol. 38, no. 2, pp. 308–320, 2017.

[46] K. YOSHIHISA, A. YOSHIMURA, Y. SHIBAMORI, K. FUCHIGAMI, and N. KUBOTA, "Polymer surface modification by using microwave plasma irradiation," Journal of Solid Mechanics and Materials Engineering, vol. 6, no. 6, pp. 654–659, 2012.

[47] S. Vyas and Y.-P. Ting, "A review of the application of ultrasound in Bioleaching and insights from sonication in (bio)chemical processes," *Resources*, vol. 7, no. 1, p. 3, 2017.

[48] "Photochemical reaction: Definition, examples, & applications," Chemistry Learner, 08-Jun-2021. [Online]. Available: https://www.chemistrylearner.com/chemical-reactions/photochemical-reaction. [Accessed: 12-Sep-2022].

[49] H. E. Bonfield, T. Knauber, F. Lévesque, E. G. Moschetta, F. Susanne, and L. J. Edwards, "Photons as a 21st century reagent," *Nature Communications*, vol. 11, no. 1, 2020.

[50] I. Langmuir, "Oscillations in ionized gases," *Proceedings of the National Academy of Sciences*, vol. 14, no. 8, pp. 627–637, 1928.

[51] T. Desmet, R. Morent, N. De Geyter, C. Leys, E. Schacht, and P. Dubruel, "Nonthermal plasma technology as a versatile strategy for polymeric biomaterials surface modification: A Review," Biomacromolecules, vol. 10, no. 9, pp. 2351–2378, 2009.

[52] G. Da Ponte, E. Sardella, F. Fanelli, R. d'Agostino, and P. Favia, "Trends in surface engineering of biomaterials: Atmospheric pressure plasma deposition of coatings for biomedical applications," *The European Physical Journal Applied Physics*, vol. 56, no. 2, p. 24023, 2011.

[53] "Absorbance measurements: BMG LABTECH," Measurements | BMG LABTECH. [Online]. Available: https://www.bmglabtech.com/en/absorbance/. [Accessed: 12-Sep-2022].

[54] "The IUPAC compendium of chemical terminology." [Online]. Available: https://dev.goldbook.iupac.org/files/pdf/green_book_2ed.pdf. [Accessed: 12-Sep-2022].

[55] D. A. Skoog, F. J. Holler, and S. R. Crouch, 'An Introduction to Infrared Spectrometry', in Principles of instrumental analysis, 6th ed., vol. 16, 34 vols, Belmont, CA: Thomson Brooks/Cole, 2007, pp. 430–454.

[56] "NMR, Mass Spectrometry, and infrared (IR) spectroscopy," *UniversalClass.com*. [Online]. Available: https://www.universalclass.com/articles/science/organic-chemistry/nmr-mass-spectrometry-and-infrared-spectroscopy.htm. [Accessed: 21-Sep-2022].

[57] D. F. Lewis, "Microscopy | Confocal Laser Scanning Microscopy," Encyclopedia of Food Microbiology, pp. 1389–1396, 1999.

[58] R. Miyazaki, C. Bertelli, P. Benaglio, J. Canton, N. De Coi, W. H. Gharib, B. Gjoksi, A. Goesmann, G. Greub, K. Harshman, B. Linke, J. Mikulic, L. Mueller, D. Nicolas, M. Robinson-Rechavi, C. Rivolta, C. Roggo, S. Roy, V. Sentchilo, A. V. Siebenthal, L. Falquet, and J. R. Meer, "Comparative genome analysis of *Pseudomonas knackmussii* b 13, the first bacterium known to degrade chloroaromatic compounds," *Environmental Microbiology*, vol. 17, no. 1, pp. 91–104, 2014.

[59] T. Narancic, M. Salvador, G. M. Hughes, N. Beagan, U. Abdulmutalib, S. T. Kenny, H. Wu, M. Saccomanno, J. Um, K. E. O'Connor, and J. I. Jiménez, "Genome analysis of the metabolically versatile *pseudomonas umsongensis* go16: The genetic basis for pet monomer upcycling into polyhydroxyalkanoates," *Microbial Biotechnology*, vol. 14, no. 6, pp. 2463–2480, 2021.

[60] C. Begot, I. Desnier, J. D. Daudin, J. C. Labadie, and A. Lebert, "Recommendations for calculating growth parameters by optical density measurements," Journal of Microbiological Methods, vol. 25, no. 3, pp. 225–232, 1996.

[61] J. P. Mofokeng, A. S. Luyt, T. Tábi, and J. Kovács, "Comparison of injection moulded, natural fibre-reinforced composites with PP and PLA as matrices," *Journal of Thermoplastic Composite Materials*, vol. 25, no. 8, pp. 927–948, 2011.

[62] S. Ali, Z. Khatri, K. W. Oh, I.-S. Kim, and S. H. Kim, "Preparation and characterization of hybrid polycaprolactone/cellulose ultrafine fibers via electrospinning," *Macromolecular Research*, vol. 22, no. 5, pp. 562–568, 2014.

[63] P. K. Singh, T. Hasan, O. Prasad, L. Sinha, K. Raj, and N. Misra, “FT-IR spectra and vibrational spectroscopy of Andrographolide,” *Spectroscopy*, vol. 20, no. 5-6, pp. 275–283, 2006.

[64] R. Lipsa, N. Tudorachi, R. N. Darie-Nita, L. Oprică, C. Vasile, and A. Chiriac, “Biodegradation of poly(lactic acid) and some of its based systems with trichoderma viride,” *International Journal of Biological Macromolecules*, vol. 88, pp. 515–526, 2016.

[65] E. C. Van Roijen and S. A. Miller, “A review of bioplastics at end-of-life: Linking experimental biodegradation studies and life cycle impact assessments,” *Resources, Conservation and Recycling*, vol. 181, p. 106236, 2022.

[66] F. Ruggero, R. C. Onderwater, E. Carretti, S. Roosa, S. Benali, J.-M. Raquez, R. Gori, C. Lubello, and R. Wattiez, “Degradation of film and rigid bioplastics during the thermophilic phase and the maturation phase of simulated composting,” *Journal of Polymers and the Environment*, vol. 29, no. 9, pp. 3015–3028, 2021.

[67] M. Ponjavic, M. S. Nikolic, J. Nikodinovic-Runic, S. Jeremic, S. Stevanovic, and J. Djonlagic, “Degradation behaviour of PCL/PEO/PCL and PCL/PEO Block Copolymers under controlled hydrolytic, enzymatic and composting conditions,” *Polymer Testing*, vol. 57, pp. 67–77, 2017.

[68] A. S. Al Hosni, J. K. Pittman, and G. D. Robson, “Microbial degradation of four biodegradable polymers in soil and compost demonstrating polycaprolactone as an ideal compostable plastic,” *Waste Management*, vol. 97, pp. 105–114, 2019.

[69] S. Jaiswal, B. Sharma, and P. Shukla, “Integrated approaches in microbial degradation of plastics,” *Environmental Technology & Innovation*, vol. 17, p. 100567, 2020.